

**This is a self-archived version of an original article. This version may differ from the original in pagination and typographic details.**

**Author(s):** Lautaoja-Kivipelto, Juulia H.; Karvinen, Sira; Korhonen, Tia-Marje; O'Connell, Thomas M; Tirola, Marja; Hulmi, Juha J.; Pekkala, Satu

**Title:** Interaction of the C2C12 myotube contractions and glucose availability on transcriptome and extracellular vesicle microRNAs

**Year:** 2024

**Version:** Accepted version (Final draft)

**Copyright:** © American Physiological Society 2023

**Rights:** In Copyright

**Rights url:** <http://rightsstatements.org/page/InC/1.0/?language=en>

**Please cite the original version:**

Lautaoja-Kivipelto, J. H., Karvinen, S., Korhonen, T.-M., O'Connell, T. M., Tirola, M., Hulmi, J. J., & Pekkala, S. (2024). Interaction of the C2C12 myotube contractions and glucose availability on transcriptome and extracellular vesicle microRNAs. *American Journal of Physiology : Cell Physiology*, 326(2), C348-C361. <https://doi.org/10.1152/ajpcell.00401.2023>

1 **Interaction of the C2C12 myotube contractions and glucose availability on**  
2 **transcriptome and extracellular vesicle microRNAs**

3 **Juulia H. Lautaoja-Kivipelto<sup>1,2\*</sup>, Sira Karvinen<sup>1</sup>, Tia-Marje Korhonen<sup>1</sup>, Thomas M.**  
4 **O'Connell<sup>3</sup>, Marja Tirola<sup>4</sup>, Juha J. Hulmi<sup>1</sup> & Satu Pekkala<sup>1</sup>**

5 <sup>1</sup>Faculty of Sport and Health Sciences, NeuroMuscular Research Center, University of  
6 Jyväskylä, Jyväskylä, 40014, Finland; [sira.m.karvinen@jyu.fi](mailto:sira.m.karvinen@jyu.fi); [tia-marje.k.korhonen@jyu.fi](mailto:tia-marje.k.korhonen@jyu.fi);  
7 [juha.hulmi@jyu.fi](mailto:juha.hulmi@jyu.fi); [satu.p.pekkala@jyu.fi](mailto:satu.p.pekkala@jyu.fi)

8 <sup>2</sup>Faculty of Medicine, Research Unit of Biomedicine and Internal Medicine, University of Oulu,  
9 Oulu, 90014, Finland: [juulia.lautaoja@oulu.fi](mailto:juulia.lautaoja@oulu.fi)

10 <sup>3</sup>Department of Otolaryngology-Head & Neck Surgery, Indiana University School of Medicine,  
11 Indianapolis, Indiana, 46202, United States; [thoconne@iu.edu](mailto:thoconne@iu.edu)

12 <sup>4</sup>Department of Biological and Environmental Science, Nanoscience Center, University of  
13 Jyväskylä, Jyväskylä, 40014, Finland; [marja.tirola@jyu.fi](mailto:marja.tirola@jyu.fi)

14 **Keywords:** electrical pulse stimulation, exercise, exerkine, skeletal muscle

15 **Running head:** Omics of the contracting C2C12 myotubes

16 \*Correspondence: Juulia H. Lautaoja-Kivipelto: [juulia.lautaoja@oulu.fi](mailto:juulia.lautaoja@oulu.fi) (ORCID: 0000-0003-  
17 2037-829X) Faculty of Sport and Health Sciences, NeuroMuscular Research Center, University  
18 of Jyväskylä, Jyväskylä, Finland and Faculty of Medicine, Research Unit of Biomedicine and  
19 Internal Medicine, University of Oulu, Oulu, Finland.

20 Supplemental Material available at:

21 Figure S1:

22 URL: <https://figshare.com/s/b82719d36229d6a241d0>

23 DOI: <https://doi.org/10.6084/m9.figshare.23918376>

24 Figure S2:

25 URL: <https://figshare.com/s/72e6eade83a688d7012f>

26 DOI: <https://doi.org/10.6084/m9.figshare.23918415>  
27 Table S1:  
28 URL: <https://figshare.com/s/b481cf99bc5dfe1f283d>  
29 DOI: <https://doi.org/10.6084/m9.figshare.23918385>  
30 Table S2:  
31 URL: <https://figshare.com/s/3105dca76c68d1563ca7>  
32 DOI: <https://doi.org/10.6084/m9.figshare.24476524>  
33 Table S3:  
34 URL: <https://figshare.com/s/0e6f57c723e13de89b27>  
35 DOI: <https://doi.org/10.6084/m9.figshare.23918475>  
36 Table S4:  
37 URL: <https://figshare.com/s/ea20ef3da4f131b0a0d3>  
38 DOI: <https://doi.org/10.6084/m9.figshare.23931369>  
39 Table S5:  
40 URL: <https://figshare.com/s/4a1f3658fff4dbb8be6a>  
41 DOI: <https://doi.org/10.6084/m9.figshare.23931375>

**42 ABSTRACT**

43 Exercise-like electrical pulse stimulation (EL-EPS) of myotubes mimics many key physiological  
44 changes induced by *in vivo* exercise. Besides enabling intracellular research, EL-EPS allows to  
45 study secreted factors, including muscle-specific microRNAs (myomiRs) carried in extracellular  
46 vesicles (EVs). These factors can participate in contraction-induced intercellular crosstalk and  
47 may mediate health benefits of exercise. However, the current knowledge of these responses,  
48 especially under variable nutritional conditions, is limited. We investigated the effects of EL-  
49 EPS on C2C12 myotube transcriptome in high and low glucose conditions by messenger RNA  
50 sequencing, while the expression of EV-carried miRNAs was analyzed by small RNA  
51 sequencing and RT-qPCR. We show that higher glucose availability augmented contraction-  
52 induced transcriptional changes and that the majority of the differentially expressed genes were  
53 upregulated. Furthermore, based on the pathway analyses, processes related to contractility and  
54 cytokine/inflammatory responses were upregulated. Additionally, we report that EL-EPS  
55 increased packing of miR-1-3p into EVs independent of glucose availability. Together our  
56 findings suggest that *in vitro* EL-EPS is a usable tool not only to study contraction-induced  
57 intracellular mechanisms, but also extracellular responses. The distinct transcriptional changes  
58 observed under variable nutritional conditions emphasize the importance of careful consideration  
59 of media composition in future exercise-mimicking studies.

**60 NEW & NOTEWORTHY**

61 The present study examined for the first time the effects of exercise-like electrical pulse  
62 stimulation administered under distinct nutritional conditions on 1) the transcriptome of the  
63 C2C12 myotubes and 2) their media containing extracellular vesicle-carried microRNAs. We  
64 report that higher glucose availability augmented transcriptional responses related especially to  
65 contractility and cytokine/inflammatory pathways. Agreeing with *in vivo* studies, we show that  
66 packing of exercise-responsive miR-1-3p was increased in the extracellular vesicles in response  
67 to myotube contractions.

## 68 INTRODUCTION

69 Exercise is known to promote health as well as to ameliorate and treat many diseases caused by  
70 sedentary lifestyle and obesity (1). During exercise skeletal muscles can modify not just their  
71 own, but also the metabolism of other organs, such as liver and adipose tissue (2). Exerkines are  
72 molecules released in response to acute and/or chronic exercise exerting their effects through  
73 endocrine, paracrine and/or autocrine pathways (3). Many organs including skeletal muscle  
74 produce and release these exerkines, such as proteins/peptides, cytokines, nucleic acids,  
75 metabolites as well as extracellular vesicles (EVs), and release them into circulation in response  
76 to exercise (2, 4). Numerous *in vivo* and *in vitro* studies have identified and validated various  
77 exerkines as well as some of their functions and target tissues (for review, see (2, 3)). Previous  
78 studies have shown that skeletal muscle specific exercise-like electrical pulse stimulation (EL-  
79 EPS) (5) of the myotubes can mimic many intra- and extracellular responses of *in vivo* exercise  
80 at the cellular (5, 6) and omics (7) levels. Additionally, we have previously shown that media  
81 glucose availability altered the metabolic responses of the C2C12 myotubes to EL-EPS (8).  
82 Because myotube gene expression is significantly impacted by the media glucose content (9, 10)  
83 and exercise responses have been reported to be affected by carbohydrate availability *in vivo*  
84 (11), it is important to examine how EL-EPS together with the variable nutritional conditions  
85 affects myotube transcriptome and regulation of the expression of genes encoding, for example,  
86 different exerkines.

87 Accumulating evidence demonstrates that EVs can encapsulate exerkines and transmit this  
88 functional cargo, such as microRNAs (miRNAs) (12, 13), via circulation to nearby and/or distant  
89 organs and tissues (14). We (15) and others (16) have shown that acute exercise induces changes  
90 in the miRNA cargo of EVs. Furthermore, some of the health-beneficial effects and adaptations  
91 of exercise have been reported to be mediated by miRNAs (17), thus making them an appealing  
92 target for biomarker research. Previous studies have shown that the levels of muscle-specific  
93 miRNAs, i.e., myomiRs, such as miR-1, miR-133a, and miR-206, are increased in the circulating  
94 EVs after exercise (12, 13). EVs are a heterogeneous group of membrane-bound particles found  
95 virtually from all biofluids *in vivo* and from conditioned cell culture media *in vitro* (17). Because  
96 the EV content can vary depending on the physiological state of the cells from which they

97 originate (18), it is important to study how nutrient availability affects EV-mediated intercellular  
98 crosstalk in response to myotube contractions. Additionally, *in vitro* approaches are needed to  
99 study the myotube-derived EVs because *in vivo* models cannot exclude the possibility that the  
100 EVs collected from the circulation, even in the presence of certain predetermined markers, are  
101 not of muscular origin.

102 This study aimed to analyze the effects of the chronic low-frequency EL-EPS together with  
103 varying media glucose content on the C2C12 myotube transcriptome and EV cargo. Several  
104 bioinformatic analyses were used to reveal the underlying mechanisms through which EL-EPS  
105 and/or availability of nutrients affect physiological responses and related pathways.

## 106 MATERIAL AND METHODS

107 **Cell culture.** The murine C2C12 myoblasts purchased from American Type Culture Collection  
108 (Manassas, VA, USA) were grown and differentiated identically as previously described in detail  
109 (8). Briefly, the myoblasts were seeded on 6-well plates and grown in high glucose (HG, 4.5 g/l,  
110 #BE12-614F, Lonza, Basel, Switzerland) containing growth medium. After reaching over 90%  
111 confluence, the fusion into myotubes was promoted by HG-containing differentiation medium  
112 (DM) (8). Representative images of the C2C12 myotubes differentiated with the identical  
113 protocol have been published previously elsewhere by us (19). The media volume per well  
114 during differentiation and experiments was 2 ml. All the experiments were performed using cells  
115 with passage number between 6-8 in a humidified environment at 37°C and 5% CO<sub>2</sub>.

116 **Exercise-like electrical pulse stimulation.** The experiments were conducted on days 4-6 post  
117 myotube differentiation by using either high or low glucose (LG, 1 g/l, #BE12-707F, Lonza)  
118 DMEM identically as previously described (8) (Figure 1). Briefly, if LG medium was used, the  
119 cells were acclimatized to LG DM from day 4 post differentiation. At day 5 post differentiation,  
120 serum- and antibiotic-free HG or LG DMEM supplemented with 2 mM L-glutamine (#25030,  
121 Gibco, Rockville, MD, USA) was added for 1 hour (20). Serum-free conditions are important not  
122 only to exclude the effects of switching to serum-free medium (20), but also to avoid co-isolation  
123 of exogenous EVs or other signal carrier particles, such as high-density lipoproteins (21). Next,  
124 the medium was removed, the myotubes were rinsed with phosphate-buffered saline (PBS,  
125 #10010, Gibco), and fresh serum-free HG or LG DMEM supplemented with 2 mM L-glutamine  
126 was added. The low-frequency EL-EPS was applied for 24 hours (1 Hz, 2 ms, 12 V) using C-  
127 Dish carbon electrodes attached to C-Pace device (Ionoptix Corporation, Milton, MA, USA).  
128 Carbon electrodes that were not attached to the C-Pace device were also placed on the control  
129 plates for the EV extraction experiments (sRNA-seq). This was done to exclude the effects of the  
130 electrodes on the EV extraction because EVs have high affinity to different types of surfaces, at  
131 least plastic (22). On day 6 post differentiation, the samples were harvested immediately after  
132 cessation of EL-EPS. To remove cell debris, media were centrifuged for 5 min at 382 x g at 4°C  
133 and the supernatants were stored at -80°C until EV extraction. Simultaneously, the myotubes

134 were washed with PBS, scraped into 340  $\mu$ l of DNA/RNA Shield (#R1100, Zymo Research,  
135 Irvine, CA, USA) and stored at room temperature (RT) until total RNA extraction.

136 **Validation of the EV isolation by nanoparticle tracking analysis and electron microscopy.**

137 The EVs were isolated using exoRNeasy serum/plasma midi kit (#77044, Qiagen, Hilden,  
138 Germany) as previously described (23). For the validation of the EV isolation protocol, 1.5 ml of  
139 media was used. Briefly, EVs were eluted by adding 140  $\mu$ l of elution buffer XE (#76214,  
140 Qiagen) followed by 5 min incubation and centrifugation for 5 min at 500 x g at RT. The  
141 collected eluate was then mixed with 360  $\mu$ l of PBS that was filtered through a 0.2  $\mu$ m filter,  
142 transferred into a 100K ultra-filter device (UFC5100, Amicon, Millipore, Darmstadt, Germany),  
143 and centrifuged for 10 min at 14 000 x g at RT. Next, the EVs were washed three times with  
144 filtered PBS to purify EVs from possible debris originating from the affinity columns and the  
145 flow-through was discarded. The concentrate was recovered by centrifugation for 2 min at 1000  
146 x g at RT according to the manufacturer's protocol. The analyses of the particle size  
147 (nanoparticle tracking analysis) and morphology (electron microscopy) were conducted at the  
148 University of Helsinki EV core (Helsinki, Finland) as previously described (23, 24). Low protein  
149 binding tubes were used whenever possible during the EV sample collection and purification.

150 **RNA extraction.** Nucleic acid extraction from the C2C12 myotube lysates stored in the  
151 DNA/RNA Shield (Zymo Research) was conducted using Chemagic 360 automated nucleic acid  
152 extraction instrument (Perkin Elmer, Boston, MA, USA). The total RNA extraction from the  
153 EVs was conducted using the exoRNeasy Serum/Plasma Midi Kit (#77144 or after  
154 discontinuation #77044, Qiagen) according to the manufacturer's protocol. Briefly about the EV  
155 RNA extraction, media from two or three wells were pooled and run through the exoRNeasy spin  
156 columns. During the RNA extraction for RT-qPCR, miRNeasy Serum/Plasma Spike-In Control,  
157 cel-miR-39 (#219610, Qiagen) was added to be used as an internal control.

158 **Library preparation and mRNA-sequencing.** The total RNA samples of the cell lysates were  
159 first treated with dsDNase (EN0771, Thermo Scientific, Waltham, MA, USA) to eliminate  
160 genomic DNA. Then, RNA concentration and integrity were measured with TapeStation



161 (Agilent Technologies, Santa Clara, CA, USA) according to the manufacturer's instructions. The  
162 average RNA integrity number (RIN) value was  $8.97 \pm 0.22$  (standard error of mean) showing  
163 low degradation of RNA. The sequencing libraries for the gene expression profiling (3' mRNA-  
164 seq) were prepared using a commercial kit (012.24A, QuantSeq 3' mRNA-Seq Library Prep Kit  
165 for Ion Torrent, Lexogen, Inc., Vienna, Austria) according to the manufacturer's protocols. After  
166 measuring the DNA concentrations with Qubit dsDNA HS Assay Kit (Invitrogen), the barcoded  
167 libraries were pooled in equimolar concentrations (5 ng of each). The pool was then purified with  
168 1.2x sparQ PureMag Beads (QuantaBio, Beverly, MA, USA) and run on a High Sensitivity  
169 D1000 Screen Tape (Agilent Technologies) to determine the quality and molarity of the pool. To  
170 bind the template to the Ion Sphere Particles (ISPs), emulsion PCR was conducted in OneTouch2  
171 instrument with Ion PGM™ Hi-Q™ OT2 Kit (Life Technologies, Carlsbad, CA, USA) following  
172 the protocol for 400-bp template according to the manufacturer's instructions. The ISPs were  
173 loaded into an Ion 318 v2 BC chip and sequencing was performed in Ion Torrent Personal  
174 Genome Machine using Ion PGM™ Hi-Q™ View Sequencing Kit (Life Technologies) similarly  
175 as described previously by us (25). To obtain a similar amount of reads from all samples, the  
176 data were pooled from two 318 v2 chips.

177 **Library preparation and small RNA-sequencing.** After the EV RNA extraction, the RIN  
178 values were not measured as small RNA (sRNA) is less sensitive for degradation and as the  
179 RNA concentration was low. The small RNA libraries for the miRNA expression profiling  
180 (sRNA-seq) were prepared using a commercial kit (#4475936, Ion Total RNA-Seq Kit v2, 12  
181 reaction kit, Thermo Fisher Scientific) according to the manufacturer's protocols with slight  
182 modifications. The products were amplified using primer pair M13\_IA 5'-  
183 TGTA AACGACGGCCAGTGGCCAAGGCG-3' and P1 5'-CCACTACGCCTCCGCTTT-3'  
184 using the Platinum Supermix and for second time using the primer P1 and the IonA\_bc\_M13  
185 adapter 5'-  
186 CCATCTCATCCCTGCGTGTCTCCGACTCAGXXXTGTA AACGACGGCCAGT-3', where  
187 XXX refers to the IonXpress barcode. The barcoded samples were pooled in equal volumes and  
188 100-140 bp sized PCR products (including 92 bp of adapter sequences) were isolated using 1.6%  
189 NuSieve agarose (Lonza) gel electrophoresis and Nucleospin Gel and PCR Cleanup (Macherey-  
190 Nagel) extraction. From this step onwards, the sequencing protocol is identical with mRNA

191 protocol described above, except that the samples were sequenced using Ion GeneStudio™ S5  
192 System with the 540 chip (Life Technologies).

193 **cDNA synthesis and real-time quantitative PCR.** For the RT-qPCR from the cell lysates,  
194 genomic DNA was eliminated, and the cDNA was synthesized using Maxima H first strand  
195 cDNA synthesis kit with dsDNase (#K1682, Thermo Fisher Scientific) according to the  
196 manufacturer's protocol. The RT-qPCR was conducted as previously described (26). The  
197 efficiency-corrected  $2^{-\Delta\Delta C_t}$  method was utilized for the RT-qPCR data analysis and *36b4* was the  
198 housekeeping gene used for normalization. The Bio-Rad Prime PCR™ Assays (Bio-Rad  
199 Laboratories, Hercules, CA, USA) used were as follows: *Cxcl1* (qMmuCED0003898), *Cxcl5*  
200 (qMmuCED0003886) and *Scml4* (qMmuCED0050877). The primer sequences for *36b4* were 5'-  
201 GGCCCTGCACTCTCGCTTTC-3' and 5'- TGCCAGGACGCGCTTGT-3' and for *Tceal7* 5'-  
202 TTGTGGCAAGGAGAAGAGAAG-3' and 5'-TGAAATTGCCTTCCAGTCGC-3'. For the RT-  
203 qPCR from the EVs, the extracted total RNA was reverse transcribed by using 12 µl of the RNA  
204 and miScript II RT Kit (#218161, Qiagen) according to manufacturer's instructions. The RT-  
205 qPCR was conducted as previously described for miRNAs and the data was analyzed by using  
206 the equation  $2^{-\Delta C_q}$  (23). The spike-in control cel-miR-39-3p was used for normalization. The  
207 miScript Primer Assays (Qiagen) used in the RT-qPCR were miR-1-3p (MS00008358), miR-  
208 133a-3p (MS00031423) and cel-miR-39-3p (MS00019789). For miR-206-3p the miScript Primer  
209 Assay was not available, and hence it was ordered separately (sequence 5'-  
210 TGGAATGTAAGGAAGTGTGTGG-3', Invitrogen, Thermo Fisher). For all the studied miRs,  
211 the sequence of the universal primer was 5'-GAATCGAGCACCAGTTACGC-3'. All the RT-  
212 qPCRs were conducted using the CFX96 Real-Time PCR Detection System combined with CFX  
213 Manager software (Bio-Rad Laboratories).

214 **Western blot.** Due to the identical culturing and methodological arrangements, the same protein  
215 lysates and Western blot protocol were used as we previously described (8). Briefly, 10 µg of  
216 protein was loaded on 4%–20% Criterion TGX Stain-Free protein gels (No. 5678094, Bio-Rad  
217 Laboratories) followed by separation using SDS-PAGE. Stain-free technology was used to  
218 control loading and for data normalization to the total protein content. After blocking, the

219 primary antibodies were probed overnight at 4°C. The primary antibodies purchased from Cell  
220 Signaling Technology (Danvers, MA, USA) and their dilutions used were as follows: p-  
221 C/EBPβ<sup>Thr235</sup> (#3084, 1:1000), p-Iκβ/α<sup>Ser32/36</sup> (#9246, 1:1000), p-IKKα/β<sup>Ser176/180</sup> (#2697, 1:1000),  
222 p-NF-κB<sup>Ser536</sup> (#3033, 1:1000), p-STAT3<sup>Tyr705</sup> (#9145, 1:1000) and STAT3 (#9139, 1:1000). The  
223 CCL2/MCP1 (NBP1-07034, 1:1000) was purchased from Novus Biologicals (Littleton, CO,  
224 USA) and MYH1E (MF 20, concentrate, 1:3000) from Developmental Studies Hybridoma Bank  
225 (Iowa City, IA, USA). The horseradish peroxidase-conjugated secondary IgG anti-mouse (1:30  
226 000) and anti-rabbit (1:10 000) antibodies were purchased from Jackson ImmunoResearch  
227 Laboratories (West Grove, PA, USA). Enhanced chemiluminescence (SuperSignal west femto  
228 maximum sensitivity substrate; Pierce Biotechnology, Rockford, IL, USA) and ChemiDoc MP  
229 device (Bio-Rad Laboratories) were used for protein visualization.

230 **Bioinformatic analyses.** The mRNA-seq data analysis steps from the initial quality check to  
231 differential expression analysis were conducted using Chipster software (<https://chipster.csc.fi/>)  
232 (27), while sRNA-seq sequence processing was conducted using CLC Genomics Workbench  
233 version 22 software (Qiagen), and further data analyses with edgeR. In more detail, for the  
234 mRNA data processing, the read quality was first analyzed using multiQC for many FASTQ  
235 files. The quality control results show Phred scores ranging from over 30 in the beginning of the  
236 sequences to about 23 at the base 300. The mean per-sequence Phred score was 27.9. and the  
237 mean sequence length was 155 bases. Next, the reads were aligned to the selected genome using  
238 STAR for single-ended reads. To count the number of aligned reads per gene, HTSeq tool was  
239 used. The average number of reads per sample was 346 191, resulting on average of 255 387  
240 reads being unambiguously mapped to the genes. The maximum read sequence number per run  
241 using the Ion Torrent PGM chips is approximately 400 000 – 560 000 per sample for 20 samples.  
242 Our average was 346 191 reads per sample showing adequate technical success. About 23% of  
243 the reads were discarded because they could be aligned to more than one region. The total  
244 number of unique genes identified was 15 273 and this data was further analyzed to determine  
245 the differentially expressed genes (DEGs) using edgeR. From this step onwards, the data were  
246 analyzed using following software's: Gene Set Enrichment Analysis (GSEA, [https://www.gsea-  
248 msigdb.org/gsea/index.jsp](https://www.gsea-<br/>247 msigdb.org/gsea/index.jsp)), Ingenuity Pathway Analysis (IPA, Qiagen,  
<https://digitalinsights.qiagen.com>) and ShinyGO (28) (<http://bioinformatics.sdstate.edu/go/>). The

249 GSEA is frequently used in exercise studies due to its low bias and ability to reveal changes in  
250 expression of a large set of genes even when the average change of gene expression is 20% or  
251 even lower (29, 30), which typically is the case with exercise (31, 32). The GSEA was conducted  
252 using fgsea R-package as previously described (33). The GSEA analysis included genes with at  
253 least 4 reads in the comparisons. When using ShinyGO, only DEGs (FDR < 0.05) from pool of  
254 the stimulated vs. pool of the non-stimulated comparison (EPS main effect) as well as all the  
255 genes as background (including more than 4 reads per sample) were input to analysis. For  
256 miRNAs, on average 2.39 M reads per sample were processed, adapter sequences were trimmed  
257 and 9-40 bp long sequences were selected for the analyses. Reads (1.1 M – 2.3 M per sample  
258 after trimming) were annotated against miRbase-Release\_v22 (*Mus musculus*), allowing length-  
259 based isomiRs, 2 additional/missing upstream and downstream bases and mismatches. In the  
260 case of sRNA-seq, miRNAs with very low expression (less than 5 samples with at least 2 counts)  
261 were filtered out. The miRNA counts were normalized by trimmed mean of M values (TMM)  
262 method (34) using edgeR-package (35). Overall, we detected 163 miRNAs from the EVs and of  
263 these, the top 50 miRNAs with the highest normalized expression were chosen for further  
264 analyses unless otherwise stated.

265 **Statistical analyses.** The statistical significance was set at Benjamini-Hochberg corrected false  
266 discovery rate (FDR) < 0.05 for multiple testing and fold change (FC) > | 1.2 | to discover DEGs.  
267 These DEG's were directed for the pathway/enrichment analyses using IPA (all comparisons)  
268 and ShinyGO (EPS main effect). For GSEA, all expressed mRNAs (which had at least 4 reads in  
269 total) were ranked in all the comparisons and used for the further GSEA. For the statistical  
270 evaluation of the main and interaction effects in sRNA-seq, RT-qPCR (cell lysates) and Western  
271 blot, the two-way multivariate analysis of variance (two-way MANOVA) was used, while the  
272 group comparisons were performed using multivariate Tukey's test (IBM SPSS Statistics,  
273 version 26 for Windows, SPSS Chicago, IL, USA). PERMANOVA analysis of normalized  
274 miRNA counts was carried out using *vegan* R-package (36) and all the 163 miRNAs. The  
275 miRNA RT-qPCR results (group comparisons as well as EL-EPS and glucose effects) were  
276 analyzed using Mann Whitney *U*-test (IBM SPSS Statistics). The extreme outliers from all the  
277 RT-qPCR analyses were removed based on Grubbs' test (<https://www.graphpad.com>). GraphPad  
278 Prism software (v10.0.2) was used to prepare the bar graphs. The Visualization and Integration

279 of Metabolomics Experiments (VIIME) software (<https://viime.org>) was used to generate the  
280 principal component analysis (PCA) score plot and the heat maps (37). Some of the plots were  
281 generated using the ggplot2 package (38) in the R programming language (version 4.3.1). The  
282 data is presented as means  $\pm$  SEM unless otherwise stated. The level of statistical significance  
283 was set at  $P < 0.05$  when FDR was not used.

## 284 RESULTS

### 285 **Higher glucose availability augmented gene expression responses after EL-EPS**

286 The effects of EL-EPS and media glucose content on the C2C12 myotube transcriptome were  
287 analyzed after the 24-hour EL-EPS by mRNA-seq. We observed eight and 66 DEGs in LG and  
288 HG conditions after EL-EPS, respectively (Figure 2A). A comparison of the combined LG and  
289 HG groups with and without EL-EPS (EPS effect) resulted in 65 DEGs (Figure 2A). Altogether,  
290 six DEGs (*Cxcl1*, *Cxcl5*, *Myh2*, *Tceal7*, *Csrp3* and *Ier3*) were shared between these three  
291 comparisons (Figure 2A). The principal component analysis (PCA) of the DEGs showed that the  
292 stimulated and non-stimulated groups were clearly separated independent of the glucose  
293 availability (Figure 2B). The heat map clustering of the DEGs show that all eight DEGs observed  
294 under LG condition were upregulated, while HG condition (50 up- and 16 downregulated DEGs)  
295 and EPS effect (50 up- and 15 downregulated DEGs) resulted in substantially more up- than  
296 downregulated DEGs (Figure 2C-E).

297 To complement the mRNA-seq results, we analyzed the expression of a few of the most up- and  
298 downregulated genes by RT-qPCR. Concordantly with the mRNA-seq results, in comparison to  
299 non-stimulated myotubes, the expression of *Cxcl1*, *Cxcl5* and *Tceal7* were higher (EPS main  
300 effects,  $P < 0.05$ ) and *Scml4* was lower (EPS main effect,  $P = 0.057$ ) in the EL-EPS-stimulated  
301 myotubes (Figure 3A-D).

### 302 **Pathways related to myotube contractibility and inflammatory responses were upregulated** 303 **in response to EL-EPS independent of the glucose availability**

304 To understand the pathways to which the identified DEGs belong, we conducted bioinformatic  
305 analyses using Gene Set Enrichment Analysis (GSEA) and Ingenuity Pathway Analysis (IPA).  
306 The GSEA analysis was performed by using the Gene Ontology Biological Processes (GOPB)  
307 database (Figure 4A-B) and for completeness, this analysis was also run with Kyoto  
308 Encyclopedia of Genes and Genomes (KEGG) and REACTOME databases (Figure S1 and Table  
309 S1). Regardless of the database used, we found that the enriched pathways after EL-EPS were  
310 mainly related to muscle architecture and contractile ability as well as cytokine and

311 inflammatory responses, independent of the media glucose availability (Figure 4A-B, Figure S1  
312 and Table S1). The IPA analyses showed that the DEGs with molecular and cellular functions  
313 related to growth, proliferation, development, movement, assembly, and organization were  
314 upregulated by EL-EPS as were intercellular signaling and interaction pathways. To complement  
315 GSEA and IPA analyses, ShinyGo analysis was conducted. By using this approach, we observed  
316 that EL-EPS induced 180 enriched GOPBs, 9 KEGG, 4 REACTOME, 9 Gene Ontology  
317 Molecular Functions and 13 Gene Ontology Cellular Component (FDR < 0.05, Table S2). With  
318 ShinyGO, many processes were similar as with GSEA and IPA in response to EL-EPS, including  
319 processes related to contractility and inflammatory response (Figure 4, Figure S1, Table S1 and  
320 Table S2).

321 Notably, we aimed to compare our previous metabolomics (8) and the present transcriptomics  
322 data to conduct trans-omic analyses using Metscape module in the Cytoscape platform  
323 (<https://cytoscape.org>). Our <sup>1</sup>H-NMR metabolomics revealed significant changes in energy  
324 metabolism related intermediates (8), while only a small number of changes in metabolic DEGs  
325 were observed in the present study. Given the paucity of metabolic transcriptional changes,  
326 MetScape analysis did not reveal interactions between the omics.

327 It is interesting to note that there were very few alterations in metabolic pathways identified in  
328 any of the datasets. Using the KEGG database, we observed an increase in the normalized  
329 enrichment score (NES) in oxidative phosphorylation in response to myotube contractions in LG  
330 conditions along with an increase in both the pentose phosphate pathway (PPP) and fructose &  
331 mannose metabolism in stimulated versus non-stimulated conditions (EPS vs. CTRL, Figure S1  
332 and Table S1). The REACTOME database revealed an increase in tricarboxylic acid cycle and  
333 respiratory electron transport in response to myotube contractions in LG conditions (Figure S1  
334 and Table S1).

335 To elucidate whether the activities of some of the pathways suggested by the bioinformatic  
336 analyses were affected at the protein level, we analyzed the myosin heavy chain 1 isoform (MF  
337 20) content and cytokine/inflammatory pathways (CCL2, p-C/EBPβ<sup>Thr235</sup> p-IKKα/β<sup>Ser176/180</sup>, p-  
338 Iκβ/α<sup>Ser32/36</sup>, p-NF-κB<sup>Ser536</sup>, p-STAT3<sup>Tyr705</sup> and STAT3) from the C2C12 myotubes after EL-EPS.  
339 Of these, when compared to the respective controls, the phosphorylation of NF-κB<sup>Ser536</sup> was

340 greater in response to EL-EPS and media glucose content (EPS main effect,  $P < 0.05$  and glucose  
341 main effect,  $P < 0.01$ , respectively, Figure 5A). The phosphorylation level or the content of  
342 CCL2, MF 20, STAT3<sup>Tyr705</sup> and total STAT3 remained unaffected (Figure 5B-E), whereas p-  
343 C/EBP $\beta$ <sup>Thr235</sup>, p-IKK $\alpha/\beta$ <sup>Ser176/180</sup> and p-I $\kappa$  $\beta/\alpha$ <sup>Ser32/36</sup> were undetected.

344 **Although media glucose content had greater effects on EV miRNAs than EL-EPS, packing**  
345 **of exercise-responsive miR-1-3p into EVs was greater after stimulation**

346 To elucidate whether miRNA-release occurs in cultured myotubes in response to EL-EPS, we  
347 collected the cell culture media, extracted the EVs and analyzed the representative samples using  
348 nanoparticle tracking analysis and electron microscopy. Based on the nanoparticle tracking  
349 analysis of the representative samples, the EV number appears to be greater in the HG media and  
350 lower in LG media of the stimulated myotubes in comparison to non-stimulated myotubes, while  
351 electron microscopy showed that the extracted EVs were of the expected size (~100 nm) in all  
352 conditions (Figure S2).

353 Next, we analyzed EV samples using sRNA-seq. Our sRNA-seq data showed that the C2C12  
354 myotubes release EVs with similar miRNA content as previously reported for *in vivo* skeletal  
355 muscle (13), including miR-206-3p, miR-1-3p and miR-133a-3p (Figure 6A, Table S2). Further  
356 data analysis of the top 50 most abundant miRNAs showed that media glucose availability had a  
357 greater effect on EV miRNA content than EL-EPS. In more detail, based on the heat map  
358 clustering, eight miRNAs were affected by media glucose content and none by the EL-EPS.  
359 More specifically, the content of miR-196a-5p, let-7f-5p and miR-26a-5p in EVs were higher in  
360 HG conditions, while miR-378c, miR-378a-3p, miR-322-5p, miR-140-3p and miR-19b-3p were  
361 higher in LG conditions (HG main effect,  $P < 0.05$ , Figure 6B). However, when we further  
362 analyzed all the 163 miRNAs using PERMANOVA analysis, we found no differences between  
363 any of the groups. In addition to sRNA-seq, we used RT-qPCR to analyze the expression of a  
364 few best-known exercise-responsive miRNAs from the EVs. Based on these analyses, we  
365 demonstrate that similar to *in vivo* exercise, myotube contractions increased the packing of  
366 specific miRNAs to the released EVs. More specifically, when compared to the respective  
367 controls, the expression of miR-1-3p was greater in response to EL-EPS (EPS effect,  $P < 0.05$ ),  
368 while miR-206-3p expression tended to be greater (EPS effect,  $P = 0.074$ ) (Figure 6C-D).



369 Numerically miR-133a-3p also increased by several fold, but due to high inter-sample variation,  
370 this result was non-significant (EPS effect,  $P = 0.242$ ) (Figure 6E).

371 **DISCUSSION**

372 The number of *in vitro* studies examining transcriptional changes after EL-EPS has increased  
373 rapidly in recent years (10, 39–45), but, to our knowledge, studies investigating the interaction  
374 between nutritional availability and the exercise responses are lacking. In the present study, we  
375 demonstrate that the contraction-induced changes in the C2C12 myotube transcriptome including  
376 reorganization of contractile units and cytokine/inflammatory responses were amplified under  
377 high glucose compared to low glucose condition. This supports our previous metabolomics  
378 findings showing that higher glucose availability augmented metabolic responses in the  
379 contracting C2C12 myotubes (8). Notably, more DEGs and pathways were up- than  
380 downregulated in response to myotube contractions, which suggests that especially under high  
381 glucose condition, the repressors of transcription were overrun by the activators. Furthermore, to  
382 the best of our knowledge, this is the first study to analyze skeletal muscle cell-derived EVs and  
383 their miRNA content after EL-EPS conducted under variable nutritional conditions. We report  
384 that several miRNAs were released from the C2C12 myotube-derived EVs and show that  
385 packing of miR-1-3p into the EVs was increased in response to myotube contractions  
386 independent of the glucose availability. Our sRNA-seq findings, however, suggest that glucose  
387 availability has more prominent effects on myotube EV miRNA content than the EL-EPS.

388 Based on the pathway analyses, the most upregulated cellular processes after EL-EPS were  
389 related to myotube contraction and structural modifications as well as cytokine and other  
390 inflammatory responses. The myotubes do not contract immediately after EL-EPS due to the lack  
391 of adequate sarcomere architecture (46). *De novo* sarcomere assembly and reorganization of the  
392 cytoskeleton are needed for the visible contractions and thus it is reasonable that muscle filament  
393 sliding, myofibril assembly, sarcomere organization, and muscle contraction pathways were  
394 upregulated in response to EL-EPS independent of the glucose availability. We showed in  
395 agreement with previous findings (10, 47) that although the gene expression of different myosin  
396 heavy chain isoforms was upregulated in response to myotube contractions especially when more  
397 glucose was available, the protein level of at least myosin heavy chain 1 isoform remained  
398 unaltered. Previously the absence of mRNA-protein correlations has been explained by the post-

399 transcriptional mechanisms needed for the mRNA to be turned into protein as well as by broad  
400 range of protein half-lives (48). The changes in myosin heavy chain isoforms may be explained  
401 by the fact that the skeletal muscle cells in the culture are at variable differentiation stages.  
402 Indeed, differentiation of the C2C12 myoblasts into myotubes has been shown to increase the  
403 expression of variable myosin heavy chain isoforms (49), while *Tceal7*, a gene previously related  
404 to improved muscle cell differentiation after muscle damage (50) was also upregulated after EL-  
405 EPS independent of the glucose availability. Moreover, EL-EPS itself may also promote  
406 differentiation and maturation of the myoblasts into myotubes (51, 52). Overall, our results  
407 suggest that repeated contractions promoted remodeling of the myotube architecture to promote  
408 contractility and possibly differentiation of the cells, especially with high glucose availability.

409 Similar to *in vivo* exercise (53), cytokine and other inflammatory pathways including response to  
410 chemokine, chemokine signaling pathway, and cytokine signaling in the immune system were  
411 enhanced after EL-EPS, and we found that this occurred independent of the glucose availability.  
412 Concordantly with the previous EL-EPS studies (39, 41, 54, 55), the expression of the members  
413 belonging to the CXC (*Cxcl1*, *Cxcl5* and *Cx3cl1*) and CC (*Ccl2* and *Ccl7*, also known as  
414 monocyte chemoattractant protein (MCP)-1 and MCP-3, respectively) chemokine families were  
415 upregulated after EL-EPS, especially with high glucose availability. Others have demonstrated  
416 that many of the CXC and CC chemokines are released into the circulation/cell culture media in  
417 response to exercise and/or muscle cell/myotube contractions (39, 54–56), probably partly via  
418  $\beta$ 2-adrenoceptor antagonist (clenbuterol)-mediated mechanisms (10). *In vivo*, cytokine and other  
419 inflammatory responses induced by acute exercise may promote the infiltration of macrophages  
420 into the skeletal muscle (57). This could enhance skeletal muscle regeneration and/or  
421 hypertrophy possibly via CXCL1, CX3CL1 and CCL2 (57–59). *In vitro*, the increased media  
422 content of CXCL1 and CXCL5 have been reported to regulate C2C12 myoblast migration and  
423 differentiation after EL-EPS (58, 60), while CCL2 release into the media in a NF- $\kappa$ B-dependent  
424 manner may promote monocyte chemoattraction *in vitro* and possibly infiltration *in vivo* (58).  
425 Supporting the potential chemokine and inflammatory signaling after EL-EPS, we observed  
426 increased phosphorylation (activation) of NF- $\kappa$ B, which supports some (39, 58), but not all (47)  
427 studies. To summarize, together our results show that EL-EPS produced similar cytokine and  
428 inflammatory responses in the skeletal muscle cells as does *in vivo* exercise and that these

429 responses were augmented by higher glucose availability. These processes are important to  
430 promote exercise-induced adaptations in the skeletal muscle *in vivo* (61), but this remains to be  
431 demonstrated *in vitro*.

432 Besides contractility and inflammation, many metabolic processes were affected by EL-EPS. We  
433 have previously reported that EL-EPS enhanced glycolysis in the myotubes based on the  
434 increased lactate production and release, especially with high glucose availability (8). Here we  
435 report concordantly that the expression of phosphofructokinase liver B-type (*Pfkl*) and pyruvate  
436 dehydrogenase kinase 1 (*Pdk1*) increased after EL-EPS. Phosphofructokinase is the key enzyme  
437 regulating glycolysis. Pyruvate dehydrogenase (PDH) promotes the conversion of pyruvate to  
438 acetyl-CoA, while enhanced PDK1 activation shifts the conversion of pyruvate towards lactate  
439 (62). Previously, the phosphorylated form of PDH has been reported to decrease in the C2C12  
440 cells after EL-EPS (42), which could increase the activity of the PDH enzyme and promote  
441 glucose oxidation in the cells, a response we previously reported after EL-EPS (8). In addition to  
442 increased lactate synthesis, lactate transport mechanisms may have been enhanced in response to  
443 myotube contractions. The solute carrier family 16 member 3 (*Slc16a3*, also known as MCT4)  
444 was upregulated in response to EL-EPS. It belongs to the monocarboxylate cotransporter (MCT)  
445 family that transport e.g., pyruvate and lactate across different membranes (63). The significance  
446 of SLC16A3 in the regulation of lactate efflux might be elevated in glycolytic cells (63) and  
447 indeed, the C2C12 myotubes can be considered relatively glycolytic cells (44). Together, the  
448 changes we have observed both at the levels of metabolites (8) and transcription in this study  
449 show that the production and probably handling of lactate were improved in the C2C12  
450 myotubes in response to EL-EPS. These observations are in accordance with human data on  
451 lactate metabolism in response to exercise (64).

452 In addition to glycolysis, pentose phosphate pathway (PPP), a parallel metabolic pathway to  
453 glycolysis, was among the overrepresented processes in response to myotube contractions. In  
454 accordance, others have previously observed contraction-induced activation of PPP in the C2C12  
455 myotubes after short-term high-frequency EL-EPS (42). They suggested that PPP activation  
456 might occur partly via reactive oxygen species (ROS) as well as Akt, extracellular regulated

457 kinase (ERK) and c-Jun N-terminal kinase (JNK) signaling (42). Notably, we have also reported  
458 increased JNK phosphorylation after EL-EPS accompanied with increased glycolytic metabolism  
459 (8). Parallel to glycolysis, activation of PPP pathway after EL-EPS may be an adaptive response  
460 to myotube contractions (42) to support the synthesis of nucleotides, certain aromatic amino  
461 acids and lipids needed for e.g., hypertrophy and membrane recovery (65). Related to PPP  
462 activation and ROS, we observed contraction-induced upregulation in the expression of  
463 superoxide dismutase 3, extracellular (*Sod3*) as well as another possibly exercise-responsive (66)  
464 redox enzyme participating in antioxidant defense, glutaredoxin (*Glx*). In accordance, ROS has  
465 been suggested to regulate transcription of antioxidant enzymes including SOD and glutathione  
466 peroxidase-1 (GPX1) after *in vivo* exercise (67). *In vitro*, others have shown that adequate  
467 protection against excessive ROS effects seems to be important to maintain myotube contractility  
468 (68) and mitochondrial function (69) during EL-EPS. Thus, future studies are recommended to  
469 examine how different EL-EPS protocols affect distinct pathways, including PPP and ROS, and  
470 what is their physiological significance.

471 The circulating miRNAs respond rapidly to exercise stimulus (70), thus making them an  
472 interesting group of potential exerkins to study not only *in vivo* but also *in vitro*. To date,  
473 miRNA studies have focused on *in vivo* exercise (for review, see(13, 17)) showing that, for  
474 example, miR-1, miR-21, miR-133, miR-155 and miR-206 could act as biomarkers of changes in  
475 exercise capacity (71). Additionally, human primary myotubes have also been previously shown  
476 to release miR-1 containing EVs in response to EL-EPS (72). Concordantly with these studies,  
477 we demonstrate that miR-1-3p as well as potentially miR-206-3p and miR-133a-3p, were  
478 increased in the EVs in response to myotube contractions independent of the media glucose  
479 availability thus suggesting these could act as potential exerkins. Among other processes, EV-  
480 derived miRNAs have been shown to promote myoblast differentiation (73). More specifically,  
481 in the C2C12 cells miR-1 enhanced myogenesis, while miR-133a promoted proliferation (74).  
482 Additionally, miR-206 has been shown to promote differentiation of the C2C12 cells (75).  
483 Beyond differentiation, miR-1 regulates e.g., mitochondrial metabolism (76, 77), while miR-  
484 133a may be an important mediator of exercise-induced adaptations in the skeletal muscle (78).  
485 miR-206 is involved in processes related, but not limited to, skeletal muscle development,  
486 growth/adaptation and regeneration (79). Although *in vivo* studies have demonstrated that the

487 number of circulating EVs increases during exercise (14), this might not be the case *in vitro* (80).  
488 We observed that the EV number was possibly increased in high, but not in low glucose  
489 condition. This suggests that myotube contractions increased the abundance of the miRNAs, but  
490 not necessarily the number of EVs. Others have shown that short-term low-frequency EL-EPS  
491 had no effects on EV size distribution or protein markers (80). Yet, as in the present study the  
492 EV number was investigated only from a representative sample and not individual samples, this  
493 needs to be verified in future studies.

494 Although both sRNA-seq and RT-qPCR identified similar miRNAs that have been linked to *in*  
495 *vivo* skeletal muscle and exercise (13, 16), our results were not fully compatible between the  
496 methods. Based on the sRNA-seq, media glucose content had greater effects on the EV-carried  
497 miRNAs than EL-EPS, while RT-qPCR showed contraction-induced increase in the miR-1-3p  
498 content, which was not confirmed by sRNA-seq. These observations are likely explained by  
499 methodological differences. Most importantly, normalization of the sRNA-seq and RT-qPCR  
500 results differ from each other (i.e., trimmed mean of M values (34) vs. spike-in cel-miR-39-3p,  
501 respectively). Furthermore, it has been previously shown that when comparing RT-qPCR to  
502 RNA-seq, 15–20% of protein coding genes were considered as non-concordant, and these genes  
503 were typically lower expressed and shorter (81). Since our study focused on sRNAs that are  
504 expressed at relatively low abundance in cell media EVs, it is likely that these factors, together  
505 with the normalization, explain the observed difference between sRNA and RT-qPCR results.  
506 Finally, most of the sRNAs identified by sRNA-seq were other than miRNAs, while RT-qPCR  
507 approach used focuses more selectively on miRNAs. To summarize the miRNA results, in  
508 agreement with the existing literature, we show that miR-1-3p content in the EVs was greater in  
509 response to EL-EPS, but more research is needed to gain a comprehensive view of  
510 miRNA/sRNA packing and EV release in response to myotube and muscle contractions.

511 *In vivo*, greater disturbances in the skeletal muscle metabolism are thought to augment exercise-  
512 induced adaptations (82). The type, intensity and duration of exercise can increase the metabolic  
513 load in the skeletal muscle and possibly lead to greater adaptations, while also nutritional  
514 strategies can be used. Indeed, carbohydrate restriction and training under low carbohydrate

515 availability and glycogen-depleted state have been shown to enhance some of the metabolic  
516 adaptations to endurance exercise, such as mitochondrial biogenesis (11). Interestingly, we report  
517 here that myotube contractions induced greater responses in the gene expression as well as  
518 previously in the metabolites (8) under HG condition. The reason for these responses may be  
519 related to the viability of the cells. Our metabolomics studies showed that glucose was almost  
520 completely depleted from the media and cells under low glucose condition (8), which may limit  
521 the metabolism of these glycolytic C2C12 cells relying heavily on carbohydrate metabolism.  
522 However, other processes, such as miRNA packing and previously reported exerkine secretion  
523 and fatty acid oxidation (8) were less affected by the media glucose content. To summarize, our  
524 current and previous (8) omics-analyses suggest that lower glucose availability may compromise  
525 contraction-induced effects on the myotubes and result in smaller metabolic perturbations.  
526 Notably, based on the analyzed markers, no unique responses or pathways were observed in low  
527 glucose condition in response to myotube contractions. Moreover, similar to metabolomics (8),  
528 the observed contraction-induced changes at the level of transcription remained either unaltered  
529 or less affected when less glucose was available. More research is warranted to study the effects  
530 of nutritional availability on myotube metabolism in response to different types of EL-EPS, e.g.,  
531 stimulation with higher frequency and/or voltage and with shorter durations. It would be  
532 important to better understand whether the glucose availability *per se* influences the contraction-  
533 induced responses in the myotubes or can the results be explained by some other mechanisms  
534 that occur due to culturing in high or low glucose containing media. Finally, as higher media  
535 glucose content augmented omics responses of the C2C12 myotubes after EL-EPS based on our  
536 present and previous (8) experiments, future studies are recommended to consider and report  
537 media composition carefully.

## 538 **LIMITATIONS OF THE STUDY**

539 Although the use of EL-EPS and myotubes as an *in vitro* exercise model is well established and  
540 we report many similar responses in the myotube gene expression and EV miRNA content as has  
541 been reported after *in vivo* exercise, this approach does not fully represent *in vivo* exercising  
542 human muscle due to the murine origin of the C2C12 cells and the lack of other cell types, such  
543 as vascular cells. Moreover, myotube cultures always contain myoblasts, but EL-EPS has been

544 mainly suggested to target myotubes. As an example, interleukin 6, a well-known exerkin, is  
545 released mainly from the differentiated and contracting myotubes (83). Thus, caution is needed  
546 when interpreting the results in relation to *in vivo* findings, especially in human studies. In the  
547 future, more time course studies are needed to better examine rapid and transient contraction-  
548 induced changes, such as cytokine bursts (84) and EV/miRNA responses (85) or delayed  
549 metabolic effects, such as myotube hypertrophy (86).

550 From the methodological point of view, EVs are complicated transport vehicles to work with due  
551 to their low abundance in the cell culture media. For example, of the small RNAs analyzed using  
552 sRNA-seq, less than 1% were miRNAs. The majority of the RNAs found in EVs were e.g.,  
553 transfer RNAs and ribosomal RNAs. Thus, the future studies are recommended to analyze not  
554 only these less well-known RNAs using e.g., PANDORA-seq (87), but also to pool media from  
555 multiple wells for one EV extraction to obtain adequate amount of starting material for the  
556 downstream analyses. Overall, despite the small sample amount, the EV miRNA results  
557 presented in this study, especially related to sRNA-seq and nanoparticle tracking analyses, are  
558 paving the way for more in-depth analysis in the future.

## 559 **CONCLUSION**

560 In conclusion, we show that the transcriptional responses of the C2C12 myotubes to EL-EPS  
561 were augmented by higher media glucose availability. Based on the pathway analyses, cellular  
562 processes including especially contractility and cytokine/inflammatory response were  
563 upregulated in response to myotube contractions independent of the media glucose content.  
564 However, only modest changes in these pathways were seen at the level of translation/protein  
565 phosphorylation. In accordance with the previous literature, we also show that EL-EPS increased  
566 myotube release and packing of miR-1-3p into the EVs, showing that as *in vivo* studies have  
567 suggested, this indeed is a potential exerkin. Yet, further studies are warranted to better  
568 understand how muscle contractions and different nutritional states regulate miRNA and EV  
569 responses. Together our results hopefully enable the development of more realistic *in vitro*  
570 exercise models.



**571 DATA AVAILABILITY**

572 The source data from mRNA (Table S4) and sRNA (Table S5) sequencing analyses (read counts)  
573 are available at:

574 Table S4:

575 URL: <https://figshare.com/s/ea20ef3da4f131b0a0d3>

576 DOI: <https://doi.org/10.6084/m9.figshare.23931369>

577 Table S5:

578 URL: <https://figshare.com/s/4a1f3658fff4dbb8be6a>

579 DOI: <https://doi.org/10.6084/m9.figshare.23931375>

**580 SUPPLEMENTAL MATERIAL**

581 The Supplemental Material is available at:

582 Figure S1:

583 URL: <https://figshare.com/s/b82719d36229d6a241d0>

584 DOI: <https://doi.org/10.6084/m9.figshare.23918376>

585 Figure S2:

586 URL: <https://figshare.com/s/72e6eade83a688d7012f>

587 DOI: <https://doi.org/10.6084/m9.figshare.23918415>

588 Table S1:

589 URL: <https://figshare.com/s/b481cf99bc5dfe1f283d>

590 DOI: <https://doi.org/10.6084/m9.figshare.23918385>

591 Table S2:

592 URL: <https://figshare.com/s/3105dca76c68d1563ca7>

593 DOI: <https://doi.org/10.6084/m9.figshare.24476524>

594 Table S3:

595 URL: <https://figshare.com/s/0e6f57c723e13de89b27>

596 DOI: <https://doi.org/10.6084/m9.figshare.23918475>

**597 ACKNOWLEDGEMENTS**

598 We acknowledge the services of university of Helsinki: EV core in FIMM Technology Centre  
599 supported by HiLIFE and Biocenter Finland for performing nanoparticle tracking analysis and  
600 electron microscopy work and Electron Microscopy Unit of the Institute of Biotechnology for  
601 providing the facilities. We appreciate the help received from Emeritus Professor Urho Kujala  
602 and Associate Professor Eija Laakkonen for the experimental procedures and reagents. We thank  
603 Elina Virtanen for the help in sequencing.

#### 604 **GRANTS**

605 The Academy of Finland (now Research Council of Finland) (Grant No. 332946 to S.K., 323063  
606 to M.T., 275922 to J.J.H, and 308042 to S.P.), Emil Aaltonen Foundation (to J.H.L-K) and the  
607 Finnish Cultural Foundation (to J.H.L-K.) funded this work. T. M. O. was supported by grants  
608 from National Institutes of Health, National Institute of Arthritis and Musculoskeletal and Skin  
609 Diseases (P01AG039355 and P30AR072581) and the Additional Ventures, Single Ventricle  
610 Research Fund. The Research Council of Finland funded profiling of the University of Jyväskylä  
611 (Profi5 301824 funding: Physical ACTivity and health during the human life-Span 2, PACTS2)  
612 and the University of Oulu (Profi6 336449 funding: Fibrobesity – Preventing fibrosis related to  
613 obesity) also supported the study.

#### 614 **AUTHOR CONTRIBUTIONS**

615 J.H.L-K., J.J.H. and S.P. conceived and designed research, J.H.L-K., performed experiments,  
616 J.H.L-K., S.K., T-M.K., T.M.O. and M.T. analyzed data, J.H.L-K., S.K. T.M.O., J.J.H. and S.P.  
617 interpreted results of experiments, J.H.L-K. and T.M.O. prepared figures, J.H.L-K. drafted  
618 manuscript, S.K., T-M.K, T.M.O., M.T., J.J.H., and S.P. edited and revised manuscript, all  
619 authors approved final version of manuscript.

#### 620 **DISCLOSURES**

621 No conflicts of interest, financial or otherwise, are declared by the authors.



## 623 REFERENCES

- 624 1. **Pedersen BK, Saltin B.** Exercise as medicine - evidence for prescribing exercise as  
625 therapy in 26 different chronic diseases. *Scand J Med Sci Sports* 25: 1–72, 2015.
- 626 2. **Severinsen MCK, Pedersen BK.** Muscle–Organ Crosstalk: The Emerging Roles  
627 of Myokines. *Endocr Rev* 41: 594–609, 2020.
- 628 3. **Chow LS, Gerszten RE, Taylor JM, Pedersen BK, van Praag H, Trappe S,  
629 Febbraio MA, Galis ZS, Gao Y, Haus JM, Lanza IR, Lavie CJ, Lee C-H, Lucia  
630 A, Moro C, Pandey A, Robbins JM, Stanford KI, Thackray AE, Villeda S,  
631 Watt MJ, Xia A, Zierath JR, Goodpaster BH, Snyder MP.** Exerkines in health,  
632 resilience and disease. *Nat Rev Endocrinol* 18: 273–289, 2022.
- 633 4. **Safdar A, Saleem A, Tarnopolsky MA.** The potential of endurance exercise-  
634 derived exosomes to treat metabolic diseases. *Nat Rev Endocrinol* 12: 504, 2016.
- 635 5. **Carter S, Solomon TPJ.** In vitro experimental models for examining the skeletal  
636 muscle cell biology of exercise: the possibilities, challenges and future  
637 developments. *Pflügers Archiv-European Journal of Physiology* 471: 413–429,  
638 2019.
- 639 6. **Nikolić N, Görgens SW, Thoresen GH, Aas V, Eckel J, Eckardt K.** Electrical  
640 pulse stimulation of cultured skeletal muscle cells as a model for in vitro exercise -  
641 possibilities and limitations. *Acta Physiologica* 220: 310–331, 2017.
- 642 7. **Lautaoja JH, Turner DC, Sharples AP, Kivelä R, Pekkala S, Hulmi JJ, Ylä-  
643 Outinen L.** Mimicking exercise in vitro: effects of myotube contractions and  
644 mechanical stretch on omics. *American Journal of Physiology-Cell Physiology* 324:  
645 C886–C892, 2023.

- 646 8. **Lautaoja JH, O’Connell TM, Mäntyselkä S, Peräkylä J, Kainulainen H,**  
647 **Pekkala S, Permi P, Hulmi JJ.** Higher glucose availability augments the  
648 metabolic responses of the C2C12 myotubes to exercise-like electrical pulse  
649 stimulation. *American Journal of Physiology-Endocrinology and Metabolism* 321:  
650 E229–E245, 2021.
- 651 9. **MacDonald TL, Pattamaprapanont P, Pathak P, Fernandez N, Freitas EC,**  
652 **Hafida S, Mitri J, Britton SL, Koch LG, Lessard SJ.** Hyperglycaemia is  
653 associated with impaired muscle signalling and aerobic adaptation to exercise. *Nat*  
654 *Metab* 2: 902–917, 2020.
- 655 10. **Fukushima T, Takata M, Kato A, Uchida T, Nikawa T, Sakakibara I.**  
656 Transcriptome Analyses of In Vitro Exercise Models by Clenbuterol  
657 Supplementation or Electrical Pulse Stimulation. *Applied Sciences* 11: 10436, 2021.
- 658 11. **Hawley JA.** Sending the Signal: Muscle Glycogen Availability as a Regulator of  
659 Training Adaptation. In: *Spiegelman B. (eds) Hormones, Metabolism and the*  
660 *Benefits of Exercise. Research and Perspectives in Endocrine Interactions.*  
661 Springer, Cham, 2017, p. 43–55.
- 662 12. **Wang H, Wang B.** Extracellular vesicle microRNAs mediate skeletal muscle  
663 myogenesis and disease. *Biomed Rep* 5: 296–300, 2016.
- 664 13. **Vechetti IJ, Valentino T, Mobley CB, McCarthy JJ.** The role of extracellular  
665 vesicles in skeletal muscle and systematic adaptation to exercise. *J Physiol* 599:  
666 845–861, 2021.
- 667 14. **Whitham M, Parker BL, Friedrichsen M, Hingst JR, Hjorth M, Hughes WE,**  
668 **Egan CL, Cron L, Watt KI, Kuchel RP.** Extracellular Vesicles Provide a Means  
669 for Tissue Crosstalk during Exercise. *Cell Metab* 27: 237–251, 2018.

- 670 15. **Karvinen S, Korhonen T, Sievänen T, Karppinen JE, Juppi H, Jakoaho V,**  
671 **Kujala UM, Laukkanen JA, Lehti M, Laakkonen EK.** Extracellular vesicles and  
672 high-density lipoproteins: Exercise and oestrogen-responsive small RNA carriers. *J*  
673 *Extracell Vesicles* 12: 12308, 2023.
- 674 16. **Siqueira IR, Palazzo RP, Cechinel LR.** Circulating extracellular vesicles  
675 delivering beneficial cargo as key players in exercise effects. *Free Radic Biol Med*  
676 172: 273–285, 2021.
- 677 17. **Nederveen JP, Warnier G, Di Carlo A, Nilsson MI, Tarnopolsky MA.**  
678 Extracellular Vesicles and Exosomes: Insights From Exercise Science. *Front*  
679 *Physiol* 11: 1757, 2021.
- 680 18. **van Niel G, D’Angelo G, Raposo G.** Shedding light on the cell biology of  
681 extracellular vesicles. *Nat Rev Mol Cell Biol* 19: 213, 2018.
- 682 19. **Lautaoja JH, Pekkala S, Pasternack A, Laitinen M, Ritvos O, Hulmi JJ.**  
683 Differentiation of Murine C2C12 Myoblasts Strongly Reduces the Effects of  
684 Myostatin on Intracellular Signaling. *Biomolecules* 10: 695, 2020.
- 685 20. **Furuichi Y, Manabe Y, Takagi M, Aoki M, Fujii NL.** Evidence for acute  
686 contraction-induced myokine secretion by C2C12 myotubes. *PLoS One* 13:  
687 e0206146, 2018.
- 688 21. **Simonsen JB.** What Are We Looking At? Extracellular Vesicles, Lipoproteins, or  
689 Both? *Circ Res* 121: 920–922, 2017.
- 690 22. **Evtushenko EG, Bagrov D v., Lazarev VN, Livshits MA, Khomyakova E.**  
691 Adsorption of extracellular vesicles onto the tube walls during storage in solution.  
692 *PLoS One* 15: e0243738, 2020.

- 693 23. **Karvinen S, Sievänen T, Karppinen JE, Hautasaari P, Bart G, Samoylenko A,**  
694 **Vainio SJ, Ahtiainen JP, Laakkonen EK, Kujala UM.** MicroRNAs in  
695 extracellular vesicles in sweat change in response to endurance exercise. *Front*  
696 *Physiol* 11: 676, 2020.
- 697 24. **Puhka M, Nordberg ME, Valkonen S, Rannikko A, Kallioniemi O, Siljander**  
698 **P, Af Hällström TM.** KeepEX, a simple dilution protocol for improving  
699 extracellular vesicle yields from urine. *European Journal of Pharmaceutical*  
700 *Sciences* 98: 30–39, 2017.
- 701 25. **Driuchina A, Hintikka J, Lehtonen M, Keski-Rahkonen P, O’Connell T,**  
702 **Juvonen R, Kuula J, Hakkarainen A, Laukkanen JA, Mäkinen E, Lensu S,**  
703 **Pietiläinen KH, Pekkala S.** Identification of Gut Microbial Lysine and Histidine  
704 Degradation and CYP-Dependent Metabolites as Biomarkers of Fatty Liver  
705 Disease. *mBio* 14, 2023.
- 706 26. **Lautaoja JH, Lalowski M, Nissinen TA, Hentilä J, Shi Y, Ritvos O, Cheng S,**  
707 **Hulmi JJ.** Muscle and serum metabolomes are dysregulated in colon-26 tumor-  
708 bearing mice despite amelioration of cachexia with activin receptor type 2B ligand  
709 blockade. *American Journal of Physiology-Endocrinology and Metabolism* 316:  
710 E852–E865, 2019.
- 711 27. **Kallio MA, Tuimala JT, Hupponen T, Klemelä P, Gentile M, Scheinin I, Koski**  
712 **M, Käki J, Korpelainen EI.** Chipster: user-friendly analysis software for  
713 microarray and other high-throughput data. *BMC Genomics* 12: 507, 2011.
- 714 28. **Ge SX, Jung D, Yao R.** ShinyGO: a graphical gene-set enrichment tool for animals  
715 and plants. *Bioinformatics* 36: 2628–2629, 2020.

- 716 29. **Mootha VK, Lindgren CM, Eriksson K-F, Subramanian A, Sihag S, Lehar J,**  
717 **Puigserver P, Carlsson E, Ridderstråle M, Laurila E, Houstis N, Daly MJ,**  
718 **Patterson N, Mesirov JP, Golub TR, Tamayo P, Spiegelman B, Lander ES,**  
719 **Hirschhorn JN, Altshuler D, Groop LC.** PGC-1 $\alpha$ -responsive genes involved in  
720 oxidative phosphorylation are coordinately downregulated in human diabetes. *Nat*  
721 *Genet* 34: 267–273, 2003.
- 722 30. **Subramanian A, Tamayo P, Mootha VK, Mukherjee S, Ebert BL, Gillette MA,**  
723 **Paulovich A, Pomeroy SL, Golub TR, Lander ES, Mesirov JP.** Gene set  
724 enrichment analysis: A knowledge-based approach for interpreting genome-wide  
725 expression profiles. *Proceedings of the National Academy of Sciences* 102: 15545–  
726 15550, 2005.
- 727 31. **Kainulainen H, Papaioannou KG, Silvennoinen M, Autio R, Saarela J,**  
728 **Oliveira BM, Nyqvist M, Pasternack A, AC't Hoen P, Kujala UM.**  
729 Myostatin/activin blocking combined with exercise reconditions skeletal muscle  
730 expression profile of mdx mice. *Mol Cell Endocrinol* 399: 131–142, 2015.
- 731 32. **Amar D, Lindholm ME, Norrbom J, Wheeler MT, Rivas MA, Ashley EA.**  
732 Time trajectories in the transcriptomic response to exercise - a meta-analysis  
733 [Online]. *Nat Commun* 12: 3471, 2021. [http://www.nature.com/articles/s41467-](http://www.nature.com/articles/s41467-021-23579-x)  
734 [021-23579-x](http://www.nature.com/articles/s41467-021-23579-x).
- 735 33. **Graber TG, Maroto R, Thompson J, Widen S, Man Z, Pajski ML, Rasmussen**  
736 **BB.** Skeletal muscle transcriptome alterations related to physical function decline in  
737 older mice. .
- 738 34. **Robinson MD, Oshlack A.** A scaling normalization method for differential  
739 expression analysis of RNA-seq data. *Genome Biol* 11: R25, 2010.



- 740 35. **Robinson MD, McCarthy DJ, Smyth GK.** edgeR: a Bioconductor package for  
741 differential expression analysis of digital gene expression data. *Bioinformatics* 26:  
742 139–140, 2010.
- 743 36. **Oksanen J, Simpson GL, Blanchet FG, Kindt R, Legendre P, Minchin PR,**  
744 **O’Hara RB, Solymos P, Stevens MHH, Szoecs E, Wagner H, Barbour M,**  
745 **Bedward M, Bolker B, Daniel Borcard D, Carvalho G, Michael Chirico M, De**  
746 **Caceres M, Sebastien Durand S, Antoniazzi Evangelista HB, FitzJohn R,**  
747 **Friendly M, Furneaux B, Hannigan G, Hill MO, Lahti L, McGlenn D,**  
748 **Ouellette M-H, Ribeiro Cunha E, Smith T, Stier A, Ter Braak CJF, Weedon J.**  
749 **vegan: Community Ecology Package [Online]. 2022. [https://CRAN.R-](https://CRAN.R-project.org/package=vegan)**  
750 **project.org/package=vegan [9 Jun. 2023].**
- 751 37. **Choudhury R, Beezley J, Davis B, Tomeck J, Gratzl S, Golzarri-Arroyo L,**  
752 **Wan J, Raftery D, Baumes J, O’Connell TM.** Viime: Visualization and  
753 Integration of Metabolomics Experiments. *J Open Source Softw* 5: 2410, 2020.
- 754 38. **Wickham H.** ggplot2: Elegant Graphics for Data Analysis [Online]. 3rd ed.  
755 Springer-Verlag New York. <https://ggplot2.tidyverse.org> [18 Jul. 2023].
- 756 39. **Scheler M, Irmeler M, Lehr S, Hartwig S, Staiger H, Al-Hasani H, Beckers J,**  
757 **Hrabé de Angelis M, Häring H-U, Weigert C.** Cytokine response of primary  
758 human myotubes in an in vitro exercise model. *American Journal of Physiology-*  
759 *Cell Physiology* 305: C877–C886, 2013.
- 760 40. **Pourteymour S, Eckardt K, Holen T, Langleite T, Lee S, Jensen J, Birkeland**  
761 **KI, Drevon CA, Hjorth M.** Global mRNA sequencing of human skeletal muscle:  
762 Search for novel exercise-regulated myokines. *Mol Metab* 6: 352–365, 2017.

- 763 41. **Sidorenko S, Klimanova E, Milovanova K, Lopina OD, Kapilevich L v,**  
764 **Chibalin A v, Orlov SN.** Transcriptomic changes in C2C12 myotubes triggered by  
765 electrical stimulation: Role of Ca<sup>2+</sup>-mediated and Ca<sup>2+</sup>-independent signaling  
766 and elevated [Na<sup>+</sup>]<sub>i</sub>/[K<sup>+</sup>]<sub>i</sub> ratio. *Cell Calcium* 76: 72–86, 2018.
- 767 42. **Hoshino D, Kawata K, Kunida K, Hatano A, Yugi K, Wada T, Fujii M, Sano**  
768 **T, Ito Y, Furuichi Y.** Trans-omic analysis reveals ROS-dependent pentose  
769 phosphate pathway activation after high-frequency electrical stimulation in C2C12  
770 myotubes. *iScience* 23: 101558, 2020.
- 771 43. **Tamura Y, Kouzaki K, Kotani T, Nakazato K.** Electrically stimulated contractile  
772 activity-induced transcriptomic responses and metabolic remodeling in C2C12  
773 myotubes: twitch vs. tetanic contractions. *American Journal of Physiology-Cell*  
774 *Physiology* 319: C1029–C1044, 2020.
- 775 44. **Abdelmoez AM, Sardón Puig L, Smith JAB, Gabriel BM, Savikj M, Dollet L,**  
776 **Chibalin A v, Krook A, Zierath JR, Pilon N.** Comparative profiling of skeletal  
777 muscle models reveals heterogeneity of transcriptome and metabolism. *American*  
778 *Journal of Physiology-Cell Physiology* 318: C615–C626, 2020.
- 779 45. **Fujita H, Horie M, Shimizu K, Nagamori E.** Microarray profiling of gene  
780 expression in C2C12 myotubes trained by electric pulse stimulation. *J Biosci*  
781 *Bioeng* 132: 417–422, 2021.
- 782 46. **Fujita H, Nedachi T, Kanzaki M.** Accelerated de novo sarcomere assembly by  
783 electric pulse stimulation in C2C12 myotubes. *Exp Cell Res* 313: 1853–1865, 2007.
- 784 47. **Lambernd S, Taube A, Schober A, Platzbecker B, Görgens SW, Schlich R,**  
785 **Jeruschke K, Weiss J, Eckardt K, Eckel J.** Contractile activity of human skeletal

- 786 muscle cells prevents insulin resistance by inhibiting pro-inflammatory signalling  
787 pathways. *Diabetologia* 55: 1128–1139, 2012.
- 788 48. **Greenbaum D, Colangelo C, Williams K, Gerstein M.** Comparing protein  
789 abundance and mRNA expression levels on a genomic scale. *Genome Biol* 4: 117,  
790 2003.
- 791 49. **Wright CR, Brown EL, Della-Gatta PA, Ward AC, Lynch GS, Russell AP.** G-  
792 CSF does not influence C2C12 myogenesis despite receptor expression in healthy  
793 and dystrophic skeletal muscle. *Front Physiol* 5: 170, 2014.
- 794 50. **Hulmi JJ, Nissinen TA, Räsänen M, Degerman J, Lautaoja JH,**  
795 **Hemanthakumar KA, Backman JT, Ritvos O, Silvennoinen M, Kivelä R.**  
796 Prevention of chemotherapy induced cachexia by ACVR2B ligand blocking has  
797 different effects on heart and skeletal muscle. *J Cachexia Sarcopenia Muscle* 9:  
798 417–432, 2018.
- 799 51. **Kawahara Y, Yamaoka K, Iwata M, Fujimura M, Kajiume T, Magaki T,**  
800 **Takeda M, Ide T, Kataoka K, Asashima M, Yuge L.** Novel Electrical  
801 Stimulation Sets the Cultured Myoblast Contractile Function to ‘On.’ *Pathobiology*  
802 73: 288–294, 2006.
- 803 52. **Faustino D, Brinkmeier H, Logotheti S, Jonitz-Heincke A, Yilmaz H, Takan I,**  
804 **Peters K, Bader R, Lang H, Pavlopoulou A, Pützer BM, Spitschak A.** Novel  
805 integrated workflow allows production and in-depth quality assessment of  
806 multifactorial reprogrammed skeletal muscle cells from human stem cells. *Cellular*  
807 *and Molecular Life Sciences* 79: 229, 2022.
- 808 53. **Kramer HF, Goodyear LJ.** Exercise, MAPK, and NF- $\kappa$ B signaling in skeletal  
809 muscle. *J Appl Physiol* 103: 388–395, 2007.

- 810 54. **Nedachi T, Fujita H, Kanzaki M.** Contractile C2C12 myotube model for studying  
811 exercise-inducible responses in skeletal muscle. *American Journal of Physiology-*  
812 *Endocrinology and Metabolism* 295: E1191–E1204, 2008.
- 813 55. **Raschke S, Eckardt K, Holven KB, Jensen J, Eckel J.** Identification and  
814 validation of novel contraction-regulated myokines released from primary human  
815 skeletal muscle cells. *PLoS One* 8: e62008, 2013.
- 816 56. **Peake JM, della Gatta P, Suzuki K, Nieman DC.** Cytokine expression and  
817 secretion by skeletal muscle cells: regulatory mechanisms and exercise effects.  
818 *Exerc Immunol Rev* 21: 8–25, 2015.
- 819 57. **Catoire M, Kersten S.** The search for exercise factors in humans. *The FASEB*  
820 *Journal* 29: 1615–1628, 2015.
- 821 58. **Miyatake S, Bilan PJ, Pillon NJ, Klip A.** Contracting C2C12 myotubes release  
822 CCL2 in an NF- $\kappa$ B-dependent manner to induce monocyte chemoattraction.  
823 *American Journal of Physiology-Endocrinology and Metabolism* 310: E160–E170,  
824 2016.
- 825 59. **Huh JY.** The role of exercise-induced myokines in regulating metabolism. *Arch*  
826 *Pharm Res* 41: 14–29, 2018.
- 827 60. **Nedachi T, Hatakeyama H, Kono T, Sato M, Kanzaki M.** Characterization of  
828 contraction-inducible CXC chemokines and their roles in C2C12 myocytes.  
829 *American Journal of Physiology-Endocrinology and Metabolism* 297: E866–E878,  
830 2009.
- 831 61. **Peake JM, Neubauer O, della Gatta PA, Nosaka K.** Muscle damage and  
832 inflammation during recovery from exercise. *J Appl Physiol* 122: 559–570, 2017.

- 833 62. **Koltai T, Reshkin SJ, Harguindey S.** *An innovative approach to understanding*  
834 *and treating cancer: targeting ph: from etiopathogenesis to new therapeutic*  
835 *avenues.* Academic Press, 2020.
- 836 63. **Jansen S, Pantaleon M, Kaye PL.** Characterization and regulation of  
837 monocarboxylate cotransporters Slc16a7 and Slc16a3 in preimplantation mouse  
838 embryos. *Biol Reprod* 79: 84–92, 2008.
- 839 64. **Brooks GA.** Lactate as a fulcrum of metabolism. *Redox Biol* 35: 101454, 2020.
- 840 65. **Wackerhage H, Vechetti IJ, Baumert P, Gehlert S, Becker L, Jaspers RT, de**  
841 **Angelis MH.** Does a Hypertrophying Muscle Fibre Reprogramme its Metabolism  
842 Similar to a Cancer Cell? [Online]. *Sports Medicine* 52: 2569–2578, 2022.  
843 <https://link.springer.com/10.1007/s40279-022-01676-1>.
- 844 66. **Lawler JM, Rodriguez DA, Hord JM.** Mitochondria in the middle: exercise  
845 preconditioning protection of striated muscle. *J Physiol* 594: 5161–5183, 2016.
- 846 67. **Scheele C, Nielsen S, Pedersen BK.** ROS and myokines promote muscle  
847 adaptation to exercise. *Trends in Endocrinology & Metabolism* 20: 95–99, 2009.
- 848 68. **Fujita H, Mae K, Nagatani H, Horie M, Nagamori E.** Effect of hydrogen  
849 peroxide concentration on the maintenance and differentiation of cultured skeletal  
850 muscle cells. *J Biosci Bioeng* 131: 572–578, 2021.
- 851 69. **Liu L, Zhang Y, Liu T, Ke C, Huang J, Fu Y, Lin Z, Chen F, Wu X, Chen Q.**  
852 Pyrroloquinoline quinone protects against exercise-induced fatigue and oxidative  
853 damage via improving mitochondrial function in mice. *The FASEB Journal* 35:  
854 e21394, 2021.

- 855 70. **Silva GJJ, Bye A, el Azzouzi H, Wisløff U.** MicroRNAs as Important Regulators  
856 of Exercise Adaptation. *Prog Cardiovasc Dis* 60: 130–151, 2017.
- 857 71. **Soplinska A, Zareba L, Wicik Z, Eyileten C, Jakubik D, Siller-Matula JM, De**  
858 **Rosa S, Malek LA, Postula M.** MicroRNAs as Biomarkers of Systemic Changes  
859 in Response to Endurance Exercise—A Comprehensive Review. *Diagnostics* 10:  
860 813, 2020.
- 861 72. **Vechetti IJ, Peck BD, Wen Y, Walton RG, Valentino TR, Alimov AP, Dungan**  
862 **CM, Van Pelt DW, von Walden F, Alkner B, Peterson CA, McCarthy JJ.**  
863 Mechanical overload-induced muscle-derived extracellular vesicles promote  
864 adipose tissue lipolysis. *The FASEB Journal* 35, 2021.
- 865 73. **Rome S, Forterre A, Bouzakri K, Mizgier ML.** Skeletal muscle-released  
866 extracellular vesicles: State of the art. *Front Physiol* 10: 929, 2019.
- 867 74. **Chen J-F, Mandel EM, Thomson JM, Wu Q, Callis TE, Hammond SM,**  
868 **Conlon FL, Wang D-Z.** The role of microRNA-1 and microRNA-133 in skeletal  
869 muscle proliferation and differentiation. *Nat Genet* 38: 228–233, 2006.
- 870 75. **Kim HK, Lee YS, Sivaprasad U, Malhotra A, Dutta A.** Muscle-specific  
871 microRNA miR-206 promotes muscle differentiation. *J Cell Biol* 174: 677–687,  
872 2006.
- 873 76. **Silver J, Wadley G, Lamon S.** Mitochondrial regulation in skeletal muscle: A role  
874 for non-coding RNAs? *Exp Physiol* 103: 1132–1144, 2018.
- 875 77. **Rodrigues AC, Spagnol AR, Frias F de T, de Mendonça M, Araújo HN,**  
876 **Guimarães D, Silva WJ, Bolin AP, Murata GM, Silveira L.** Intramuscular

- 877 Injection of miR-1 Reduces Insulin Resistance in Obese Mice. *Front Physiol* 12,  
878 2021.
- 879 78. **Nie Y, Sato Y, Wang C, Yue F, Kuang S, Gavin TP.** Impaired exercise tolerance,  
880 mitochondrial biogenesis, and muscle fiber maintenance in miR-133a-deficient  
881 mice. *The FASEB Journal* 30: 3745–3758, 2016.
- 882 79. **Ma G, Wang Y, Li Y, Cui L, Zhao Y, Zhao B, Li K.** MiR-206, a Key Modulator  
883 of Skeletal Muscle Development and Disease. *Int J Biol Sci* 11: 345–352, 2015.
- 884 80. **Bydak B, Pierdoná TM, Seif S, Sidhom K, Obi PO, Labouta HI, Gordon JW,**  
885 **Saleem A.** Characterizing Extracellular Vesicles and Particles Derived from  
886 Skeletal Muscle Myoblasts and Myotubes and the Effect of Acute Contractile  
887 Activity [Online]. *Membranes (Basel)* 12: 464, 2022. [https://www.mdpi.com/2077-](https://www.mdpi.com/2077-0375/12/5/464)  
888 [0375/12/5/464](https://www.mdpi.com/2077-0375/12/5/464).
- 889 81. **Everaert C, Luypaert M, Maag JL V., Cheng QX, Dinger ME, Hellemans J,**  
890 **Mestdagh P.** Benchmarking of RNA-sequencing analysis workflows using whole-  
891 transcriptome RT-qPCR expression data. *Sci Rep* 7: 1559, 2017.
- 892 82. **Hawley JA, Lundby C, Cotter JD, Burke LM.** Maximizing Cellular Adaptation  
893 to Endurance Exercise in Skeletal Muscle. *Cell Metab* 27: 962–976, 2018.
- 894 83. **Farmawati A, Kitajima Y, Nedachi T, Sato M, Kanzaki M, Nagatomi R.**  
895 Characterization of contraction-induced IL-6 up-regulation using contractile C2C12  
896 myotubes. *Endocr J* 60: 137–147, 2013.
- 897 84. **Shirasaki Y, Yamagishi M, Suzuki N, Izawa K, Nakahara A, Mizuno J, Shoji**  
898 **S, Heike T, Harada Y, Nishikomori R.** Real-time single-cell imaging of protein  
899 secretion. *Sci Rep* 4: 4736, 2014.

- 900           85.   **Russell AP, Lamon S, Boon H, Wada S, Güller I, Brown EL, Chibalin A v.,**  
901           **Zierath JR, Snow RJ, Stepto N, Wadley GD, Akimoto T.** Regulation of miRNAs  
902           in human skeletal muscle following acute endurance exercise and short-term  
903           endurance training. *J Physiol* 591: 4637–4653, 2013.
- 904           86.   **Tarum J, Folkesson M, Atherton PJ, Kadi F.** Electrical pulse stimulation: an in  
905           vitro exercise model for the induction of human skeletal muscle cell hypertrophy. A  
906           proof-of-concept study. *Exp Physiol* 102: 1405–1413, 2017.
- 907           87.   **Shi J, Zhang Y, Tan D, Zhang X, Yan M, Zhang Y, Franklin R, Shahbazi M,**  
908           **Mackinlay K, Liu S, Kuhle B, James ER, Zhang L, Qu Y, Zhai Q, Zhao W,**  
909           **Zhao L, Zhou C, Gu W, Murn J, Guo J, Carrell DT, Wang Y, Chen X, Cairns**  
910           **BR, Yang X, Schimmel P, Zernicka-Goetz M, Cheloufi S, Zhang Y, Zhou T,**  
911           **Chen Q.** PANDORA-seq expands the repertoire of regulatory small RNAs by  
912           overcoming RNA modifications. *Nat Cell Biol* 23: 424–436, 2021.
- 913



914 **FIGURE LEGENDS**

915 **FIGURE 1.** Schematic presentation of the study design.

916 **FIGURE 2.** The effects of exercise-like electrical pulse stimulation (EL-EPS, EPS in the figure)  
917 and media glucose availability on the C2C12 myotube transcriptome. (A) Venn graph of the  
918 differentially expressed genes (DEGs). (B) Principal component analysis (PCA) of the DEGs.  
919 The read counts were used to create the PCA score plot. The heat map categorization of the  
920 DEGs after EL-EPS in (C) low and (D) high glucose (LG and HG, respectively) condition as  
921 well as (E) in the pool of the stimulated vs. non-stimulated samples (EPS vs. CTRL). The dashed  
922 lines cluster the DEGs that respond similarly to EL-EPS in each comparison. The heat map  
923 categorization is based on *k*-means clustering and the coloring on the *z*-scores. In A, false  
924 discovery rate < 0.05 and fold change > | 1.2 |. N = 5 per group except in EPS vs. CTRL, N =  
925 10 per group.

926 **FIGURE 3.** Complementary analysis of the mRNA-seq results after exercise-like electrical pulse  
927 stimulation (EL-EPS, EPS in the figure) by RT-qPCR. The mRNA expression of (A) *Cxcl1*, (B)  
928 *Cxcl5*, (C) *Tceal7*, and (D) *Scml4*. For the analysis of EL-EPS and media glucose content (EPS  
929 and HG main effects, respectively) and their interaction effect, the two-way MANOVA was  
930 used. The group comparisons were analyzed with multivariate Tukey's test. In the figures, the  
931 values are presented as normalized to low glucose (LG) = 1 or high glucose (HG) = 1. N = 3–4  
932 per group. \* = P < 0.05 and \*\*\* = P < 0.001, respectively.

933 **FIGURE 4.** The top ten (A) over- and (B) underrepresented pathways after exercise-like  
934 electrical pulse stimulation (EL-EPS, EPS in the figure) on the C2C12 myotubes. The  
935 bioinformatic gene set enrichment analysis (GSEA) pathway analyses were conducted by using  
936 Gene Ontology Biological Processes (GOBP) database. Data in the figures is categorized by  
937 normalized enrichment scores (NES) and -Log<sub>10</sub> of false discovery rate (FDR) values. Note that  
938 FDR < 0.05 equals >1.3 in -Log<sub>10</sub> (FDR) scale and for clarity, the X- and Y-axes do not start at  
939 zero for the plots. Bold = pathway related to contractility and/or muscle structure, italics =

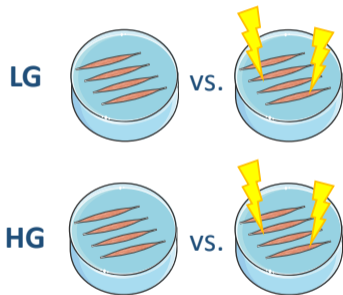
940 pathway related to cytokine and other inflammatory responses. N = 5 per group except for a pool  
941 of stimulated vs. non-stimulated (EPS vs. CTRL) comparison, N = 10 per group.

942 **FIGURE 5.** The effects of the exercise-like electrical pulse stimulation (EL-EPS, EPS in the  
943 figure) and media glucose content on cytokine and inflammatory signaling as well as on  
944 contractile protein. (A) Phosphorylated NF- $\kappa$ B<sup>Ser536</sup>, (B) phosphorylated STAT3<sup>Tyr705</sup> and total  
945 STAT3, (C) CCL2 and (D) myosin heavy chain 1 (MF 20). (E) Representative blots. –, no  
946 stimulation; +, stimulation. In the figures, the values are presented as normalized to low glucose  
947 (LG) = 1 or high glucose (HG) = 1. The two-way MANOVA was used to analyze EL-EPS and  
948 media glucose content effects (EPS and HG main effects, respectively) and their interaction  
949 effect, whereas group comparisons were analyzed with multivariate Tukey's test. N = 6 per  
950 group.

951 **FIGURE 6.** The effects of the exercise-like electrical pulse stimulation (EL-EPS, EPS in the  
952 figure) on the extracellular vesicle (EV) microRNA (miRNA) content. A) Top 10 miRNAs in the  
953 C2C12 cell-derived EVs based on small RNA sequencing. The proportions represent the  
954 percentage of the top 50 miRNAs analyzed. All four groups were pooled for the analysis. B) The  
955 heat map categorization of the EV-derived miRNAs in the pool of the high and low glucose  
956 samples (HG vs. LG, respectively). The dashed line clusters the miRNAs that respond similarly  
957 to the media glucose content. The heat map categorization is based on *k*-means clustering and the  
958 coloring on the *z*-scores. The expression of (C) miR-1-3p, (D) miR-206-3p and (E) miR-133a-3p  
959 analyzed by RT-qPCR. The values are presented as normalized to LG or HG = 1. In B, the two-  
960 way MANOVA was used to analyze EL-EPS and media glucose content effects (EPS and HG  
961 main effects, respectively) and their interaction effect, whereas group comparisons were  
962 analyzed with multivariate Tukey's test. In C-D, EPS and HG effects as well as the group  
963 comparisons were conducted using Mann Whitney *U*-test. In A, N = 20, in B, N = 10 per group  
964 (HG vs. LG) and in C-E, N = 5–6 per group.

## EXPERIMENTS & COMPARISONS

±EL-EPS (24h, 1 Hz, 2 ms, 12 V)



Low (LG, 1g/L) OR high (HG, 4.5 g/L)  
glucose media

## COLLECTION

Myotubes    Media

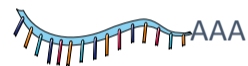


RNA,  
proteins

EVs

## ANALYSES

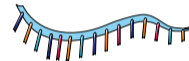
Myotube  
mRNA seq (N = 5)



EV sRNA seq (N = 5)  
EV miRNA RT-qPCR (N = 5-6)

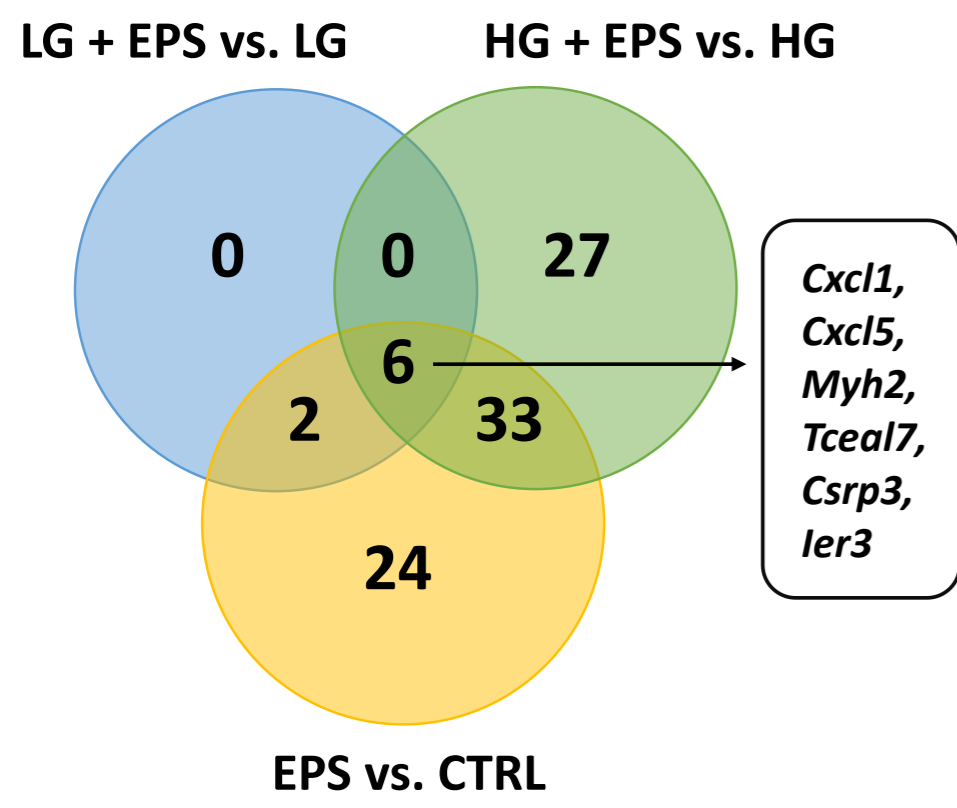
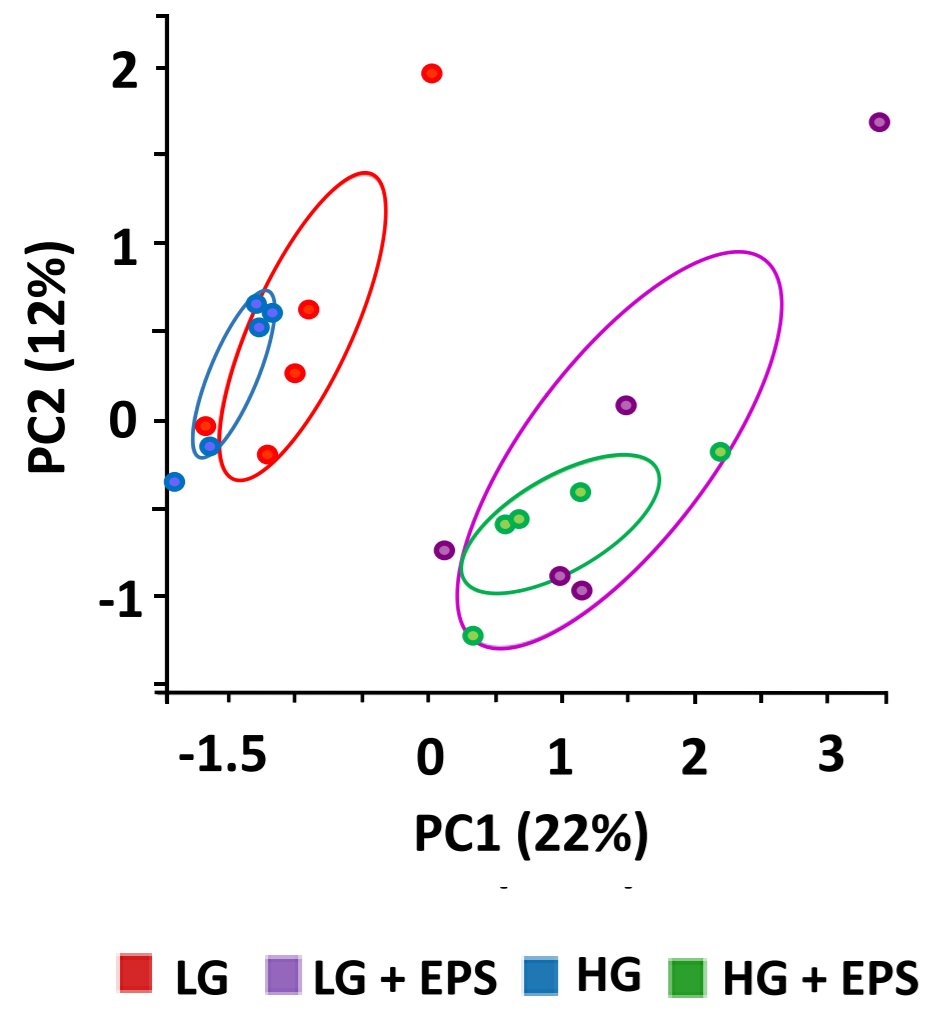
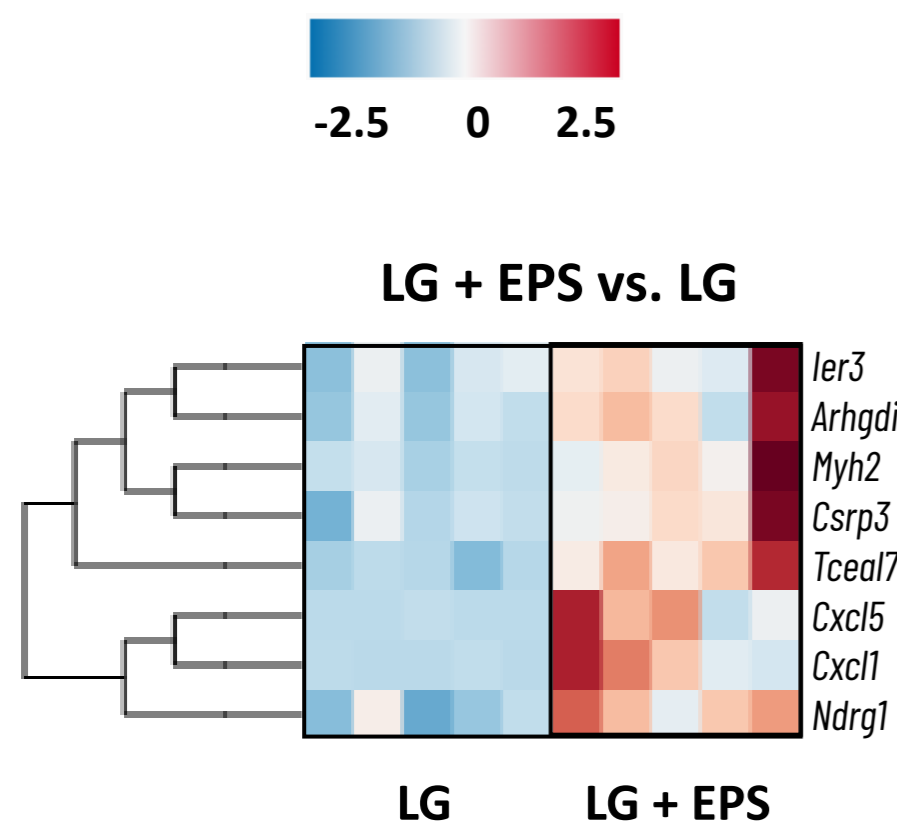
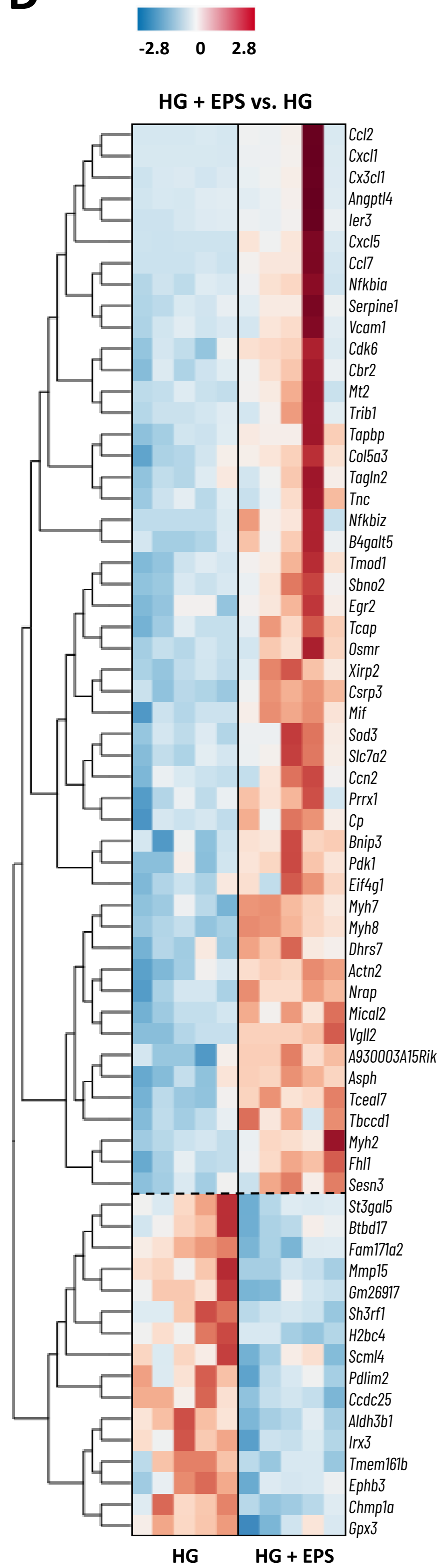
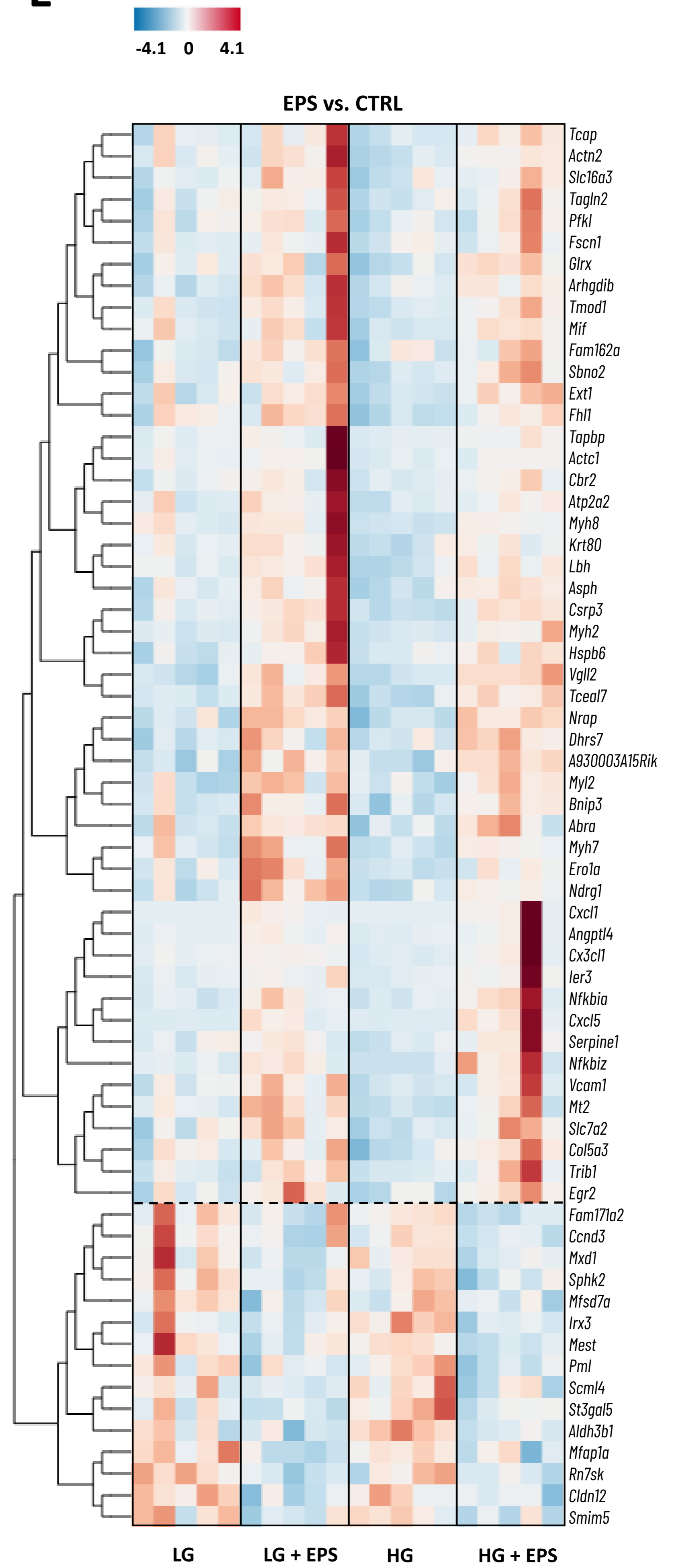


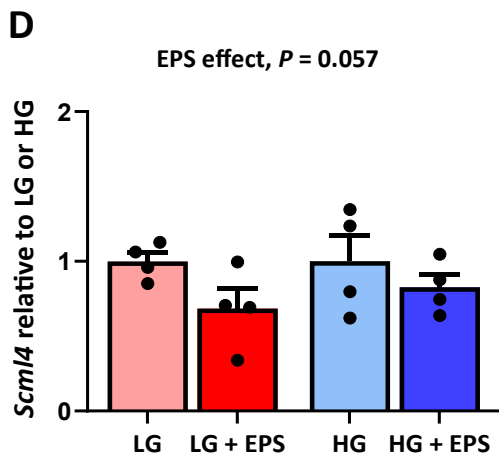
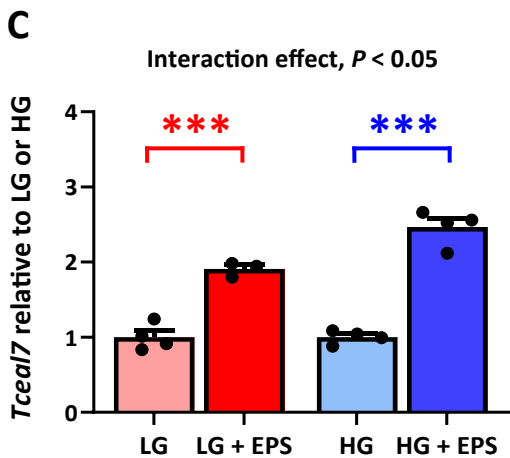
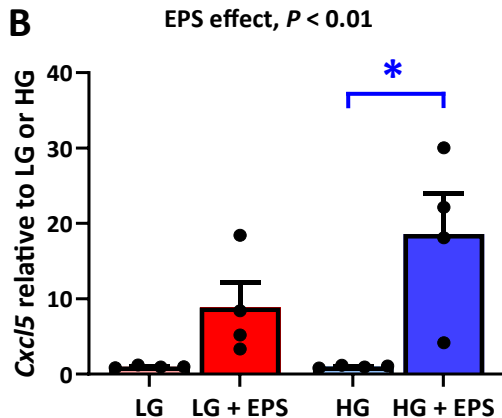
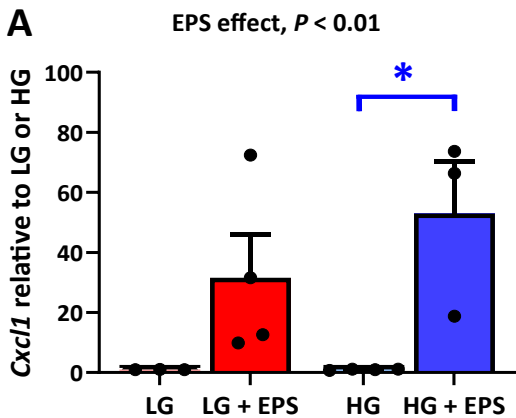
Myotube  
RT-qPCR (N = 3-4)



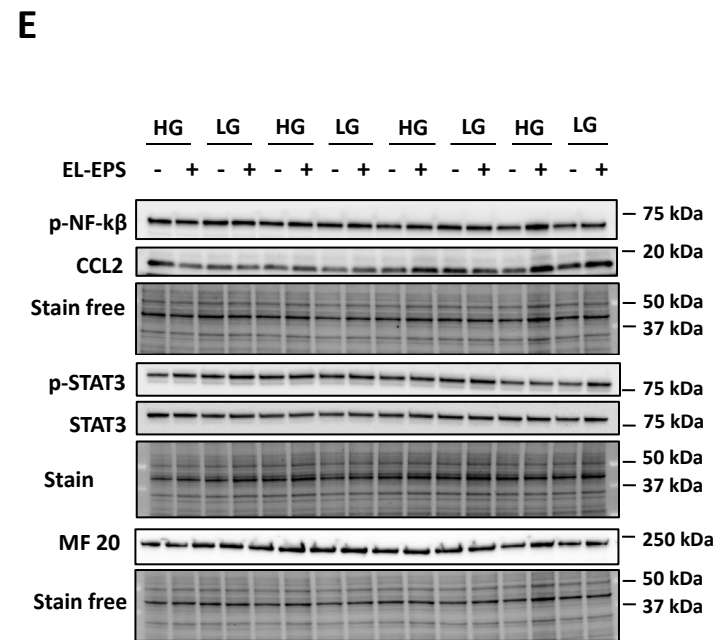
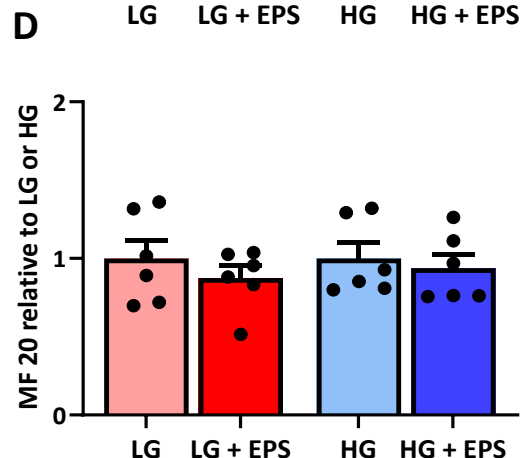
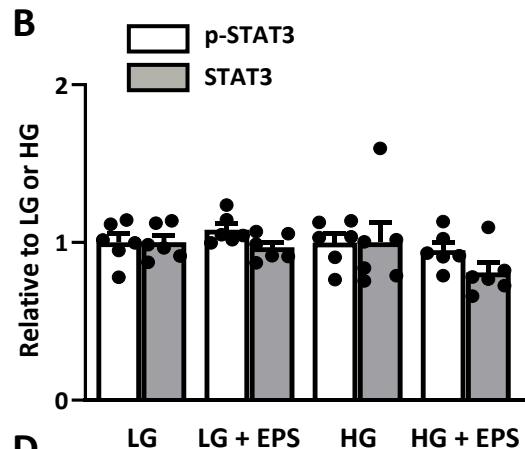
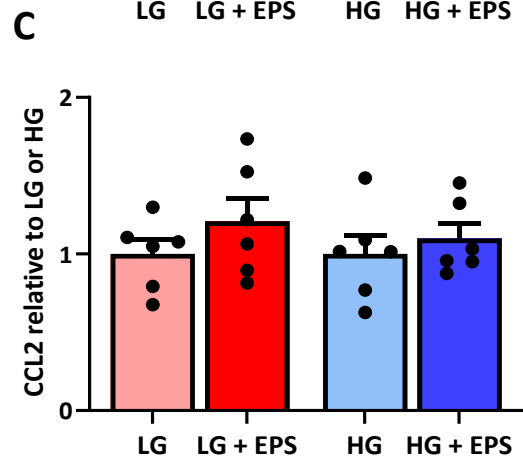
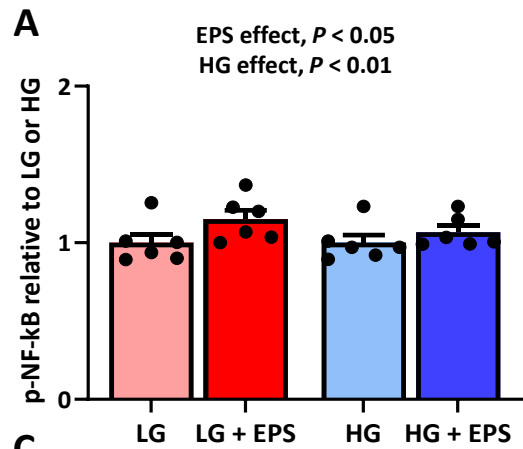
Myotube  
Western blot (N = 6)

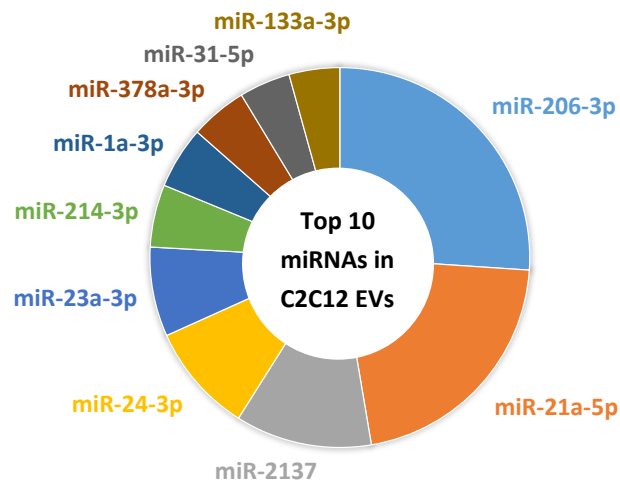
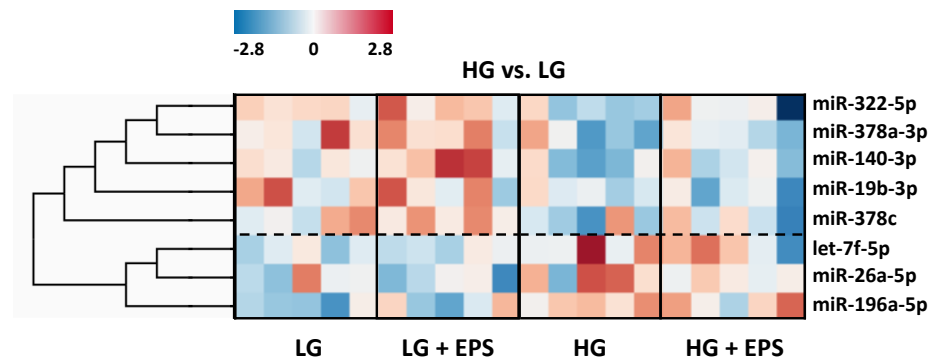
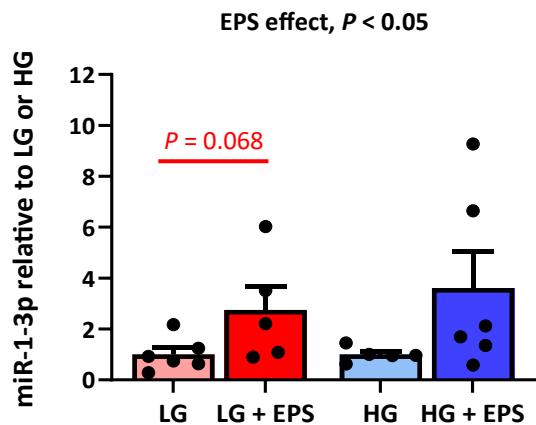
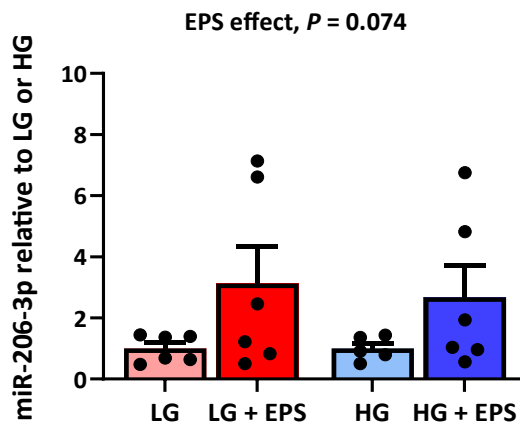
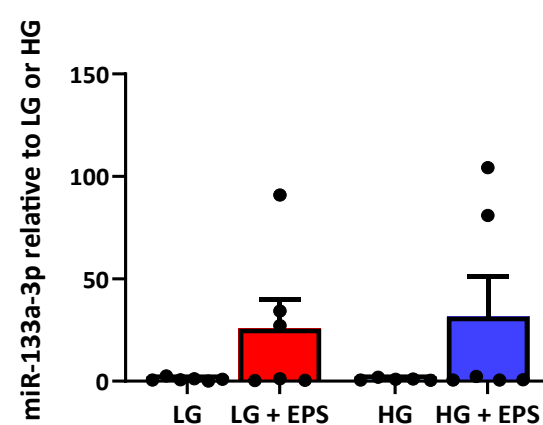


**A****B****C****D****E**





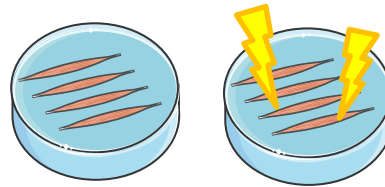


**A****B****C****D****E**

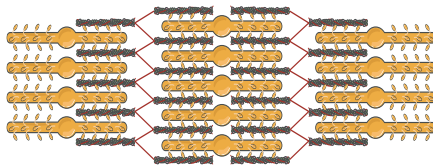


# Higher glucose availability augments transcriptional responses but not miR-1-3p packing into extracellular vesicles in the contracting C2C12 myotubes

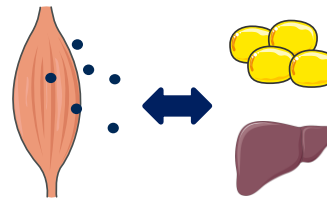
High (4.5 g/l) OR low (1 g/l)  
glucose media



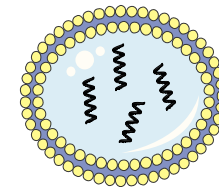
± 24h, 1 Hz, 2 ms, 12 V  
electrical pulse stimulation



Genes related to  
contractility



Genes related to cytokine and  
inflammatory response



miR-1-3p packing into  
extracellular vesicles



**CONCLUSION: Independent of glucose availability, myotube contractions promote packing of miR-1-3p into extracellular vesicles thus supporting its' role as a potential exerkine**